

The bright end of the colour-magnitude relation of cluster galaxies

Noelia Jiménez^{1,2*}, Sofía A. Cora^{1,2}, Lilia P. Bassino^{1,2}, Tomás E. Tecce^{2,3} and Analía V. Smith Castelli^{1,2}

¹*Facultad de Ciencias Astronómicas y Geofísicas de la Universidad Nacional de La Plata, and Instituto de Astrofísica de La Plata (CCT La Plata, CONICET, UNLP), Observatorio Astronómico, Paseo del Bosque S/N, B1900FWA La Plata, Argentina*

²*Consejo Nacional de Investigaciones Científicas y Técnicas, Rivadavia 1917, C1033AAJ Buenos Aires, Argentina*

³*Instituto de Astronomía y Física del Espacio, CC. 67 Suc. 28, C1428ZAA Ciudad de Buenos Aires, Argentina*

Accepted. Received; in original form

ABSTRACT

We investigate the physical processes involved in the development of the red sequence (RS) of cluster galaxies by using a combination of cosmological N -body simulations of clusters of galaxies and a semi-analytic model of galaxy formation. Results show good agreement between the general trend of the simulated RS and the observed colour-magnitude relation (CMR) of early-type galaxies in different magnitude planes. However, in many clusters, the most luminous galaxies ($M_R \sim M_V \sim M_{T_1} \lesssim -20$) depart from the linear fit to observed data, as traced by less luminous ones, displaying almost constant colours. With the aim of understanding this particular behaviour of galaxies in the bright end of the RS, we analyze the dependence with redshift of the fraction of stellar mass contributed to each galaxy by different processes, i.e., quiescent star formation, and starbursts triggered by disc instability and merger events. We find that the evolution of galaxies in the bright end since $z \approx 2$ is mainly driven by minor and major dry mergers, while minor and major wet mergers are relevant in determining the properties of less luminous galaxies. Since the most luminous galaxies have a narrow spread in ages ($1.0 \times 10^{10} \text{ yr} < t < 1.2 \times 10^{10} \text{ yr}$), their metallicities are the main factor that affects their colours. Their mean iron abundances are close to the solar value and have already been reached at $z \approx 1$. This fact is consistent with several observational evidences that favour a scenario in which both the slope and scatter of the CMR are in place since $z \approx 1.2$. Galaxies in the bright end reach an upper limit in metallicity as a result of the competition of the mass of stars and metals provided by the star formation occurring in the galaxies themselves and by the accretion of merging satellites. Star formation activity in massive galaxies (stellar mass $M_\star \gtrsim 10^{10} M_\odot$) that takes place at low redshifts contribute with stellar components of high metallicity, but the fraction of stellar mass contributed since $z \approx 1$ is negligible with respect to the total mass of the galaxy at $z = 0$. On the other hand, mergers contribute with a larger fraction of stellar mass ($\approx 10 - 20$ per cent), but the metallicity of the accreted satellites is lower by ≈ 0.2 dex than the mean metallicity of galaxies they merge with. The effect of dry mergers is to increase the mass of galaxies in the bright end, without significantly altering their metallicities. Hence, very luminous galaxies present similar colours that are bluer than those expected if recent star formation activity were higher, thus giving rise to a break in the RS. These results are found for simulated clusters with different virial masses ($10^{14} - 10^{15} h^{-1} M_\odot$), supporting the idea of the universality of the CMR in agreement with observational results.

Key words: galaxies: clusters: general - galaxies: formation - galaxies: evolution

1 INTRODUCTION

It is now well established that galaxies follow a bimodal distribution in the colour-magnitude plane, separated into

* E-mail: njimenez@fcaglp.unlp.edu.ar

a tight ‘red sequence’ (RS) and a ‘blue cloud’. The RS mostly consists of gas-poor galaxies with low levels of star formation (SF), prototypically early-type galaxies (ETGs), whereas late-type galaxies are typical objects of the blue cloud.

The colour-magnitude relation (CMR) of ETGs can be understood as a mass-metallicity relation. The more luminous (and therefore more massive) galaxies in this relation have deep potential wells, capable of retaining the metals released by supernovae events and stellar winds. The CMR seems to be quite universal, since it is followed by galaxies in the field as well as in groups and clusters (e.g. Visvanathan & Sandage 1977; Sandage & Visvanathan 1978; Reda et al. 2004; López-Cruz et al. 2004; Reda et al. 2005; de Rijcke et al. 2009), but with a larger fraction of red galaxies being in denser environments.

There is controversy on which are the mechanisms responsible for the evolution of galaxies to the RS. The physical processes invoked can be classified in internal and external. The former include passive stellar evolution and disc instabilities, while the latter involve galaxy-galaxy interactions and mergers (Lin et al. 2010; Robaina et al. 2010), and environmental effects such as fast gravitational interactions (‘galaxy harassment’, Moore et al. 1999), removal of the hot gas reservoir (‘strangulation’ or ‘starvation’, Larson et al. 1980; Balogh et al. 2000; Kawata & Mulchaey 2008) and ram pressure stripping of galactic gas (Lanzoni et al. 2005; Roediger 2009; Tecce et al. 2010).

Studying the evolution of the slope and scatter of the CMR provides constraints on the SF history of ETGs. Bower, Kodama & Terlevich (1998) find that the observed CMR scatter in local clusters can be reproduced if galaxies are assumed to form the bulk of their stellar content at early epochs ($z > 1$), with a subsequent moderate mass growth driven by merger events and residual SF activity. This scenario is consistent with hierarchical models of galaxy formation. In this context, using semi-analytical modelling, Menci et al. (2008) obtain a narrow RS for cluster galaxies, already defined by $z \approx 1.2$. At a similar redshift, Kaviraj et al. (2005) find that the slope of the CMR of cluster galaxies changes appreciably with respect to its present value, although the evolution of the slope in the redshift range $0 < z < 0.8$ is negligible taking into account the errors.

Detailed observations of the CMR of cluster galaxies (see Mei et al. 2009, and references therein) show no significant evolution of the zero point, slope and scatter of the CMR out to $z \approx 1.3$. In contrast with these results, Stott et al. (2009) find from optical and near-infrared observations of cluster galaxies an evolution of the CMR slope between $z \approx 0.5$ and the present epoch, which they attribute to the infall of galaxies into the cluster core that are being transformed into RS galaxies.

Hydrodynamical simulations have also been used to analyse the properties of the CMR at $z = 0$. Saro et al. (2006) evaluate the impact of the stellar initial mass function (IMF), finding that the Salpeter IMF allows to recover both the slope and the normalization of the CMR for galaxies in cluster-sized haloes. From the analysis of simulations of galaxy groups and clusters, Romeo et al. (2008) conclude that the shape of the RS is mainly determined by the specific SF in all environments. These authors find that evol-

ing galaxies move towards a ‘dead’ sequence soon after they have almost stopped the bulk of their SF. Fainter galaxies in clusters keep a significant amount of SF out to very recent epochs, and are thus distributed more broadly around the RS.

A linear relation has generally been used to fit the correlation between luminosity and colour of the CMR, from giant to dwarf ellipticals. However, the scatter of these relations increases at lower luminosities, as becomes evident from observations of several clusters (Coma, Secker et al. 1997; Perseus, Conselice et al. 2003; Fornax, Hilker et al. 2003, Karick et al. 2003, Mieske et al. 2007; Hydra, Misgeld et al. 2008; Virgo, Lisker et al. 2008; Antlia, Smith Castelli et al. 2008).

Some of these relations seem to be consistent with a change of slope from the bright to the faint end. As an example, this kind of fit has already been suggested by de Vaucouleurs (1961) for the Virgo cluster, and confirmed later by Ferrarese et al. (e.g. 2006). More recently, based on Sloan Digital Sky Survey (SDSS) imaging data, Janz & Lisker (2009) found, also for Virgo, a non-linear relation that can be described by a ‘S’ shape over the whole range of magnitudes, with the brightest galaxies ($-21 \lesssim M_B \lesssim -19$) having an almost constant colour. In the case of the Hydra cluster, Misgeld et al. (2008) fit a linear relation to its CMR, but a change of slope is evident for the brightest galaxies in that cluster.

Additional evidence of a tilt towards bluer colours at the bright end of the RS arises from studies of large samples of galaxies in the SDSS (e.g. Baldry et al. 2004, 2006; Skelton et al. 2009). The results of Skelton et al. (2009) were obtained for the local RS averaged over all environments. Baldry et al. (2006) examined the dependence of the fit (using a ‘S’-shaped combination of straight line plus a hyperbolic tangent function) to the mean positions of both the RS and blue cloud, and found that unlike the fractions of red galaxies, the fits to the RS do not vary strongly with environment.

The detachment of the bright end from the general trend denoted by the linear fit to the CMR of cluster galaxies motivates our study. The CMR constitutes one of the major tools to test galaxy formation models since galactic evolution is evidenced by it. Our aim is to contribute to the understanding of the physical processes behind the development of the RS in galaxy clusters, and the special behaviour of its bright end.

Recent observations support strong evolution with cosmic time in the structural properties of the most massive (stellar mass $M_\star \gtrsim 10^{11} M_\odot$) spheroid-like galaxies. Size measurements of ellipticals at high redshift ($z \gtrsim 1.5$) reveal that these objects are much smaller (by factors ~ 2 to ~ 4) than their local counterparts of comparable stellar mass (Daddi et al. 2005). This result was subsequently confirmed by several studies, although the most massive ETGs ($M_\star \gtrsim 2.5 \times 10^{11} M_\odot$) seem to have reached their internal and dynamical structure earlier and faster than lower mass ETGs at the same redshift, as discussed by Mancini et al. (2010). On the other hand, a mild evolution in velocity dispersion is found for massive galaxies (Cenarro & Trujillo 2009). On average, the velocity dispersion and surface mass density of massive galaxies at high redshift are similar to those of the most dense local ETG

(Cappellari et al. 2009). These observational evidences suggest that inside-out growth scenarios are plausible, in which the compact high redshift galaxies make up the centres of normal nearby ellipticals (van Dokkum et al. 2010).

From samples of galaxy pairs obtained from different surveys, it is found that present-day massive ETGs undergo, on average, ~ 0.5 major mergers since $z \sim 0.6 - 0.7$ (Bell et al. 2006b; Robaina et al. 2010). These mergers generally occur between galaxies which are already on the RS, thus involving ETGs containing little cold gas and dust (Whitaker & van Dokkum 2008; McIntosh et al. 2008). These dissipationless (gas-poor, thus called ‘dry’) major mergers are an important channel for the formation and evolution of the brightest cluster galaxies (BCGs) (Liu et al. 2009). However, the rate of dry major mergers is too low to fully explain the formation of spheroidal (and RS) galaxies since $z \sim 1$ (Bundy et al. 2009). Minor dry mergers would favour the growth of BCGs as inferred from the evolution of their velocity dispersion-stellar mass relation (Bernardi 2009). The minor merger hypothesis also appears to be plausible for early-type galaxies at intermediate redshifts ($0.1 < z < 0.8$) as shown by Nierenberg et al. (2011) who find that ETGs are typically surrounded by several satellite galaxies. Minor mergers are also probably responsible for the size evolution of massive ETGs (Bezanson et al. 2009). Besides, Kaviraj et al. (2011) demonstrate that the low-level of star formation activity in the ETG population at intermediate redshift is likely to be driven by minor mergers.

The influence of mergers on the evolution of ETGs inferred from observational data is in agreement with predictions obtained from models of galaxy formation. Using semi-analytic modelling techniques, Khochfar & Burkert (2003) find that the last major merger of present-day bright elliptical galaxies ($M_B \lesssim -21$) occurs preferentially between bulge-dominated galaxies. Major mergers are responsible for doubling the stellar mass at the massive end of the RS since $z \sim 1$ (Eliche-Moral et al. 2010). On the other hand, Bournaud, Jog & Combes (2007) study the effect of multiple minor mergers on ETG evolution by using a N -body simulation finding that repeated minor mergers can form elliptical galaxies without major mergers events, which are less frequent than minor mergers at moderate redshift. Remnants of these multiple mergers develop global properties that depend more on the total mass accreted during mergers than on the mass ratio of each merger. This result is also supported by hydrodynamic simulations (e.g. Naab et al. 2007, 2009) which suggest that the growth of massive galaxies ($M_* \gtrsim 10^{11} M_\odot$) by a large series of minor mergers becomes more important than the growth via major mergers; minor mergers may thus be the main driver for the late evolution of sizes and densities of ETGs. Another possible physical mechanism responsible for the size evolution of ETGs is the expulsion of a substantial fraction of the initial baryons, still in gaseous form, by quasar activity (Fan et al. 2010).

From semi-analytic modelling, Khochfar & Silk (2006) find that massive galaxies at high redshifts form in gas-rich mergers, whereas galaxies of the same mass at low redshifts form from gas-poor mergers. These considerations allow them to reproduce the observed size-redshift evolution of massive spheroidal objects. Dissipation associated with large gas fractions is the most important factor determining spheroid sizes, as found by Hopkins et al. (2009) us-

ing high resolution hydrodynamic simulations. Complementary, also using semi-analytic models, De Lucia & Blaizot (2007) find that later ($z < 0.5$) minor dry mergers play an important role in the mass assembly of BCGs, which acquire half of their mass via accretion of smaller galaxies.

It is clear that different types of mergers have a strong impact on the evolution of ETGs, affecting their morphological and kinematical properties, as well as their star formation history. As has been described, many works have been devoted to study these aspects but only a few have analysed in detail the role of mergers in the development of the CMR (e.g. Skelton et al. 2009; Bernardi et al. 2010). In particular, by using a toy model combined with galaxy merger trees extracted from a semi-analytic model, Skelton et al. (2009) find that the tilt towards bluer colours of the bright end of the RS of local early-type galaxies can be explained by the higher fraction of dry mergers suffered by bright galaxies with respect to fainter ones. Galaxy colour is not expected to change during dry mergers, since there is no associated SF. Galaxies then move along the CMR as the mass of the system increases, with their colour remaining fixed (Bernardi et al. 2007).

In this work, we investigate this issue in detail using the semi-analytic model of galaxy formation and evolution SAG (acronym for Semi-Analytic Galaxies; Lagos, Cora & Padilla 2008, hereafter LCP08), which is combined with hydrodynamical cosmological simulations of galaxy clusters by Dolag et al. (2005). We focus our study on galaxies lying on the RS, which are selected by a colour criterion. The samples thus obtained mostly include early type galaxies, making our conclusions valid for the understanding of the development of the CMR of ETGs. Thus, we hereafter use the term RS to refer to colour-selected galaxies from our simulations, and the term CMR to refer to observed relations for ETGs.

The tilt in the bright end of the RS emerges naturally from the model once it has been calibrated to recover numerous observed galaxy properties, both locally and at high redshift. We quantify the contribution to the mass and metal content of galaxies located in the RS given by quiescent SF from the cold gas available in the galaxy disc, starbursts triggered by disc instability and merger events, and the stellar mass accreted from satellite galaxies during mergers, which are identified as minor/major and wet/dry ones.

This paper is organised as follows. In Section 2, we briefly describe the semi-analytic model used in this work and give details of the cluster simulations. Section 3 presents the comparison between the simulated RS and observed CMR followed by early-type cluster galaxies in different magnitude planes, and the analysis of the luminosity-metallicity relation followed by galaxies in the RS. Section 4 describes the formalism used to quantify the contribution of different processes to the mass and metallicity of galaxies; the corresponding results are presented and discussed. Finally, in Section 5 we summarize our main findings.

2 HYBRID MODEL OF GALAXY FORMATION AND EVOLUTION

In this work, we focus our analysis on the RS of cluster galaxies. We investigate the development of the RS by applying

a numerical technique which combines cosmological non-radiative N -Body/SPH (Smoothed Particle Hydrodynamics) simulations of galaxy clusters in a concordance Λ Cold Dark Matter universe and a semi-analytic model of galaxy formation and evolution. In this hybrid model, the outputs of the cosmological simulation are used to construct merger histories of dark matter (DM) haloes and their embedded substructures, which are then used by the semi-analytic code to generate the galaxy population. In this Section we briefly describe the hybrid model.

2.1 Simulated galaxy clusters

We consider two sets of simulated galaxy clusters, C14 and C15, which contain clusters with virial masses in the ranges $\simeq (1.1 - 1.2) \times 10^{14} h^{-1} M_{\odot}$ and $\simeq (1.3 - 2.3) \times 10^{15} h^{-1} M_{\odot}$, respectively. The clusters in the C14 set are named g1542, g3344, g6212, g676 and g914, whereas those in C15 are g1, g8, g51 (see Dolag et al. 2005, for details). These clusters have been initially selected from a DM-only simulation with a box size of $480 h^{-1}$ Mpc (Yoshida et al. 2001), for a cosmological model characterized by $\Omega_m = 0.3$, $\Omega_{\Lambda} = 0.7$, $H_0 = 70 \text{ km s}^{-1} \text{ Mpc}^{-1}$, $\Omega_b = 0.039$ for the baryon density parameter, and $\sigma_8 = 0.9$ for the normalization of the power spectrum. The Lagrangian regions surrounding the selected clusters have been re-simulated at higher mass resolution by applying the ‘Zoomed Initial Condition’ technique (Tormen et al. 1997) and the Tree-SPH GADGET-2 code (Springel et al. 2005). The mass resolution is the same for all simulations, with masses of DM and gas particles $m_{\text{dm}} = 1.13 \times 10^9 h^{-1} M_{\odot}$ and $m_{\text{gas}} = 1.69 \times 10^8 h^{-1} M_{\odot}$, respectively. As for the force resolution, the Plummer-equivalent gravitational softening is fixed at $\epsilon = 5 h^{-1}$ kpc in physical units at redshift $z \leq 5$, while it switches to comoving units at higher redshifts taking a value of $\epsilon = 30 h^{-1}$ kpc.

Although the simulations are hydrodynamical, we only use the kinematical information provided by DM particles in order to identify DM haloes. To this aim, we consider that DM particles have their masses increased to its original value, since gas was introduced in the high-resolution region by splitting each parent particle into a gas and a DM particle. Dark haloes are first identified as virialized particle groups by a friends-of-friends (FOF) algorithm. The SUBFIND algorithm (Springel et al. 2001) is then applied to these groups in order to find self-bound DM substructures, which we call subhaloes. Subhaloes are the sites of galaxy formation, and their merger trees are built by extracting from the simulations all subhaloes with 10 or more bound DM particles, since smaller ones are dynamically unstable (Kauffmann et al. 1999).

2.2 Semi-analytic model SAG

The semi-analytic model SAG used here is based on that described by Lagos et al. (2008). The physical processes considered in this model are the cooling of hot gas as a result of radiative losses, quiescent star formation, and starbursts during disc instability events and galaxy mergers. Feedback from supernova explosions and active galactic nuclei (AGN) are also considered. The mass of hot gas available in a halo is determined at each simulation output on which the semi-

analytic model is applied. This mass is defined as the baryonic fraction of the virial mass of the halo minus the total mass of baryons in the form of cold gas and stars and the mass of black holes already present within the halo. The model tracks the circulation of metals between the different baryonic components, that is, hot diffuse gas, cold gas and stars, taking into account the mass evolution of different chemical elements (Cora 2006). The version of SAG used in this work incorporates the more detailed calculation of disc galaxy scale radii described in Tecce et al. (2010).

After tuning the free parameters involved in the different physical processes considered, the model is able to reproduce several observational constraints simultaneously, such as galaxy luminosity functions, relations between central black hole mass and other properties of the host bulge, quasar luminosity function, stellar mass functions at different redshifts, and mass-metallicity, colour-magnitude and disc size-luminosity relations (see LCP08 and Tecce et al. 2010 for details).

During their evolution, galaxies can acquire stellar mass by SF, either in quiescent form by converting their cold gas into stars, or in starbursts which can be triggered by disc instability events or galaxy mergers. During mergers, a galaxy’s stellar mass also increases due to the stars accreted from the merging satellite. In SAG, as in many other semi-analytic codes, only central galaxies have cooling flows; the cold gas accreted is assumed to settle into the galactic disc. A galaxy’s mass can subsequently be reduced through recycling due to stellar winds and supernovae explosions. The latter also reduce the amount of cold gas available for further SF through energy feedback. AGN activity also injects energy into the hot phase and decreases the flow of cooling gas into the galaxy, thus regulating SF as well.

The complex combination of all these processes is reflected in the resulting metallicities and luminosities of galaxies. In the present study, we track the increase of galaxy mass considering, separately, the contribution of new stars formed during SF episodes of different types (quiescent mode and starburst modes) and stars accreted from satellite galaxies during mergers. SAG considers both major and minor mergers, and in this work we also identify them as either wet or dry mergers. In the following, we give a short description of the parameters that characterize different types of mergers, and refer the reader to LCP08 for details on quiescent SF and disc instability events.

2.3 Galaxy mergers and starbursts

In a hierarchical scenario of structure formation, mergers of galaxies are a natural consequence of the mergers of DM haloes in which they reside, and play an important role in determining the mass and morphology of galaxies. The galaxy catalogue is built up by applying the semi-analytic model to the detailed DM subhalo merger trees extracted from the cluster simulations. After the identification of DM substructures within FOF groups, the largest subhalo in a FOF group is assumed to host the central galaxy of the group, located at the position of the most bound particle of the subhalo. These galaxies are designated as *central* galaxies. Central galaxies of other smaller subhaloes contained within the same FOF group are referred to as *halo* galaxies. The subhaloes hosting these galaxies are still intact after

falling into larger structures. There is a third group of galaxies generated when two subhaloes merge and the galaxy of the smaller one becomes a satellite of the remnant subhalo. We assume that these *satellite* galaxies merge with their corresponding subhalo central galaxy on a dynamical friction time-scale.

Mergers are classified as *major* or *minor* according to the ratio between the baryonic mass (stellar plus cold gas mass) of the accreted satellite galaxy and of the central galaxy, $f_{\text{merge}} = M^{\text{sat}}/M^{\text{central}}$. A major merger occurs when $f_{\text{merge}} > 0.3$. Otherwise, we are in the presence of a minor merger.

In the case of a major merger, all stars present in the merging galaxies are rearranged into a spheroid. Additionally, all the cold gas available in the remnant is consumed in a starburst as a result of the perturbation introduced by the merging satellite. This perturbation drives the cold gas into the bulge component of the remnant, where it is completely transformed into stars. Thus, major mergers lead to the creation of an elliptical galaxy.

On the other hand, during minor mergers all the stars of the merging satellite galaxy are added to the spheroid of the remnant, whereas the stellar disc of the accreting galaxy remains unaltered. The presence of a starburst during a minor merger depends on the gas mass fraction of the disc of the central galaxy, $f_{\text{ColdGas}}^{\text{central}} = M_{\text{ColdGas}}^{\text{central}}/M_{\text{disc}}^{\text{central}}$, where $M_{\text{disc}} = M_{\text{Stellar}} - M_{\text{Bulge}} + M_{\text{ColdGas}}$, M_{Stellar} is the total stellar mass of the galaxy, M_{Bulge} is the mass of the bulge (formed only by stars), and M_{ColdGas} is the cold gas content of the galaxy. If $f_{\text{ColdGas}}^{\text{central}} > f_{\text{gas,minor}}$, all the cold gas in the merging galaxies is assumed to undergo a starburst; stars formed in this fashion are then added to the bulge of the remnant. The inclusion of the minor merger starburst threshold ($f_{\text{gas,minor}}$) is motivated by the suggestion of Hernquist & Mihos (1995) that gas-rich discs should be susceptible to bursts triggered by the accretion of small satellites. Malbon et al. (2007) consider this SF channel in a semi-analytic code; varying the minor merger starburst threshold with respect to the value adopted by them, we find that we are able to reproduce the observed luminosity function with $f_{\text{gas,minor}} = 0.6$ (as done in LCP08). This type of merger is considered a *minor wet merger* since it leads to SF. In this case, the stellar mass of the central galaxy is increased by the new stars formed and by the stellar content of the accreted satellite galaxy.

On the contrary, if $f_{\text{ColdGas}}^{\text{central}} < f_{\text{gas,minor}}$ then no burst occurs, and we classify it as a *minor dry merger*. Furthermore, bursts do not occur if the satellite is much less massive than the central galaxy ($f_{\text{merge}} < f_{\text{burst}}$, with $f_{\text{burst}}=0.05$), regardless of the amount of gas in the central disc. Since this type of minor merger does not trigger starbursts, it is also considered a minor dry merger. The choice of these parameters allows us to reconcile observational data with the properties of the galactic populations given by SAG.

For the sake of our study, we also need to classify major mergers as either wet or dry. This classification does not affect how SAG works, and is only of interest for the identification of different types of processes that contribute to galaxy formation. Then, once we have identified a major merger, we classify it as wet or dry depending on the gas fraction of the disc of the remnant. Then, if $f_{\text{ColdGas}}^{\text{remnant}} < f_{\text{gas,major}}$ the major merger is dry, and it is wet otherwise. We adopt the value

$f_{\text{gas,major}} = 0.4$; further discussion regarding the choice of this parameter will be given in Section 4.

3 COLOUR-MAGNITUDE RELATION

On the basis of the results obtained by applying our semi-analytic code SAG to the sets of simulated galaxy clusters C14 and C15, we are able to construct the corresponding RS, whose bright end is mostly populated by ETGs. In the simulations, galaxies belonging to the RS are selected according to the empirical redshift-dependent separation between colour sequences given by Bell et al. (2004), based on the bimodal distribution of observed galaxy colours out to $z \approx 1$. In this way, galaxies redder than

$$(U - V) = 1.15 - 0.31z - 0.08(M_V - 5\log h + 20), \quad (1)$$

for $0 < z < 1$, are considered as belonging to the RS. In the following, we adopt $z = 0$ to obtain simulated RS at the present epoch and compare them with observed CMRs of ETGs. As we will be basically dealing with the CMR slope but not with its zero-point, we do not need to convert observational data from absolute into apparent magnitudes and vice-versa. In the model, neither magnitudes are influenced by extinction nor the colours are affected by reddening.

3.1 Slopes of the colour-magnitude relations in different bands

Our semi-analytic model provides the magnitudes of galaxies in the Johnson-Morgan system. In order to compare with observed data, they have to be transformed to other photometric systems. Fig. 1 shows the RS obtained for one of the more massive simulated clusters (C15.3) in three different colour-magnitude planes: R vs. $U - R$, R vs. $(B - R)$, and T_1 vs. $(C - T_1)$. We also show the RS of a less massive cluster (C14.2) in the T_1 vs. $(C - T_1)$ plane in the right bottom panel. The R magnitude is in the Cousins system, while the C and T_1 magnitudes correspond to the Washington photometric system. The $(C - T_1)$ integrated colour has proved to be quite sensitive to metallicity for old, single stellar populations like globular clusters (e.g., see Harris & Harris 2002; Forte et al. 2007), while the $(U - R)$ integrated colour is age sensitive. Besides, the RS in the V vs. $(V - I)$ plane is also considered in the analysis, but not shown in this figure.

The R and I magnitudes in the Johnson-Morgan system are transformed into the Cousins system through the relations given by Fukugita et al. (1995) for ETGs. The photometric conversion from Johnson-Morgan V minus Cousins I colours into the Washington $(C - T_1)$ ones is performed through the transformation $(V - I) = 0.49(C - T_1) + 0.32$, given by Forbes & Forte (2001) for globular clusters, under the assumption that ETGs are mainly old stellar systems as well. Finally, T_1 magnitudes are obtained from the Cousins R ones by applying the relation $R - T_1 \sim -0.02$, given by Geisler (1996).

It can be clearly seen from Fig. 1 that the simulated RS of the C15 cluster, in the three colour-magnitude planes, present a break with brighter galaxies detached from the general trend denoted by the fainter ones. This break occurs at approximately the same magnitude in the different systems ($M_R^{\text{break}} \sim M_V^{\text{break}} \sim M_{T_1}^{\text{break}} \approx -20$; galaxy mass

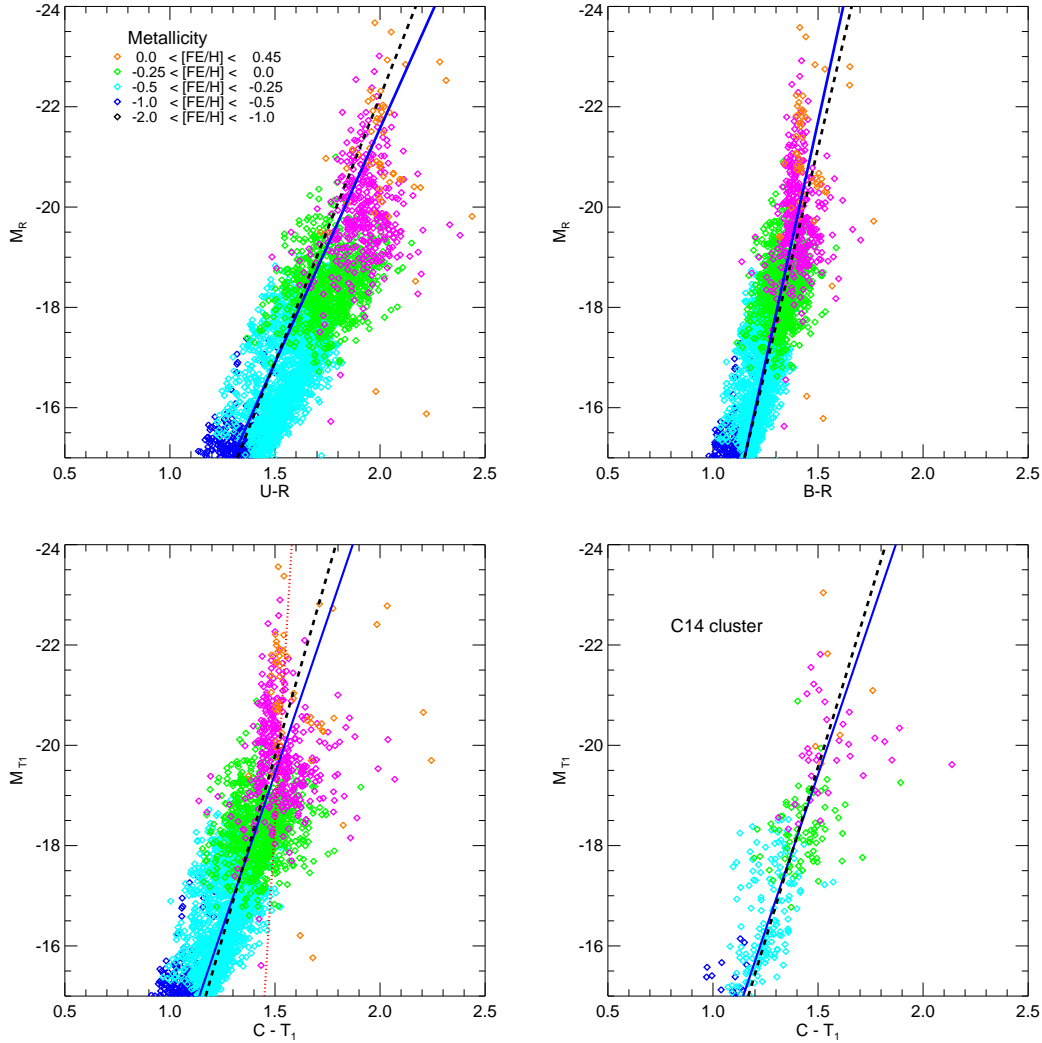


Figure 1. RS obtained from the semi-analytic model SAG applied to the C15_3 and C14_2 simulated galaxy clusters (see Table 1) in different photometric systems: R vs. $(U - R)$ and R vs. $(B - R)$ for C15_3 cluster (top), and T_1 vs. $(C - T_1)$ for C15_3 cluster (bottom left) and C14_2 cluster (bottom right). Symbols are coloured according to the iron abundance of the simulated galaxies. Least-squares fits to the faint end of the simulated RS and to the whole relation are represented by blue solid lines and black dashed lines, respectively. The fit to the bright end of the simulated RS of the C15 cluster is also shown in the plane T_1 vs. $(C - T_1)$ (red dotted line).

of $\sim 10^{10} M_{\odot}$), being more evident in the Washington system, with brighter galaxies displaying an almost constant colour ($C - T_1 \approx 1.5$). Taking such break as a reference, we will refer hereafter to the galaxies brighter/fainter than the magnitude of the break as the ‘bright/faint end’ of the RS.

Two fits are performed to the simulated RS in each photometric system, considering the whole relation and the faint end only. These fits are shown in Fig. 1 for the C15_3 cluster and for C14_2 cluster as black dashed and blue solid lines, respectively. Table 1 presents the slopes of these least-squares fits performed to the RS of the eight simulated clusters described in Subsection 2.1. Note that the slopes depicted in Table 1, designated as b in the following analysis, correspond to RS where the colour is the independent variable. In order to compare with those obtained from observed CMRs, we will have to invert the ‘observed’ slopes ($1/b$) in the cases

that CMRs are calculated taking the colour as the dependent variable (i.e. as if the diagrams displayed in Fig. 1 were rotated 90°).

With regard to the observed CMRs, a wide cluster sample is presented by López-Cruz et al. (2004), who study the CMRs of 57 low-redshift cluster galaxies, with different richness, cluster types and X-ray luminosities. The fits to the CMRs are performed in the $(B - R)$ vs. R plane (see their table 1), from which we calculate an average slope $1/b_{BR} = -0.051 \pm 0.002$, or $b_{BR} = -19.61$ to compare with our simulations. This falls within the range of values presented in Table 1 for the corresponding ‘all CMR’ fits.

Misgeld et al. (2008) fit the CMR of the early-type dwarf galaxy sample ($M_V > -17$) of Hydra I cluster in the $(V - I)$ vs. V plane, and get a slope $1/b_{VI} = -0.039$ (rms error of the fit equal to 0.12), or $b_{VI} = -25.64$. They

Table 1. Slopes calculated from least-squares fits to both the faint end of the RS and the whole relation, for the different simulated clusters in several photometric bands.

Cluster	R vs. $B - R$		V vs. $V - I$		T_1 vs. $C - T_1$		R vs. $U - R$	
	Faint end	All	Faint end	All	Faint end	All	Faint end	All
C14_1 (g1542)	-16.92	-19.90	-20.12	-25.22	-10.79	-12.29	-8.55	-9.85
C14_2 (g3344)	-18.55	-20.00	-19.97	-27.85	-12.24	-13.77	-12.24	-13.77
C14_3 (g6212)	-19.23	-20.88	-24.65	-30.37	-12.36	-13.80	-9.58	-10.07
C14_4 (g676)	-17.43	-20.38	-26.47	-28.95	-11.45	-13.83	-8.75	-9.79
C14_5 (g914)	-16.39	-18.99	-21.48	-25.31	-10.47	-12.35	-8.30	-9.25
C15_1 (g1)	-18.10	-21.36	-24.78	-29.72	-11.48	-13.96	-9.00	-10.32
C15_2 (g8)	-18.11	-20.69	-24.12	-28.84	-11.55	-13.71	-9.15	-10.21
C15_3 (g51)	-18.96	-21.78	-25.57	-31.19	-12.38	-14.62	-9.33	-10.48

also estimate the slope of the CMR for Local Group dwarf ellipticals (dE) and dwarf spheroidals (dSph) in the same colour-magnitude plane as $1/b_{VI} = -0.038$ (rms of the fit 0.09), or $b_{VI} = -26.32$. Still in the same plane, a slope $1/b_{VI} = -0.033 \pm 0.004$, or $b_{VI} = -30.30$, is given by Mieske et al. (2007) for the dE galaxy sample ($M_V > -17$) in the Fornax cluster. Misgeld et al. (2009) analyse the CMR followed by dwarf ETGs in the Centaurus cluster and obtain $1/b_{VI} = -0.042$ (rms of the fit 0.10), or $b_{VI} = -23.81$. Except for the slightly lower value from Mieske et al., all the slopes are within the range covered by those of the ‘faint end’ fits listed in Table 1.

The Perseus cluster is studied by de Rijcke et al. (2009) with HST/ACS data; they present a global CMR that includes several other groups and clusters, obtaining a common fit with slope $1/b_{VI} = -0.033 \pm 0.004$, or $b_{VI} = -30.30$, which is also in agreement with ‘all CMR’ values from Table 1.

Smith Castelli et al. (2008) obtained the CMR of ETGs located in the central region of the Antlia cluster, using the Washington photometric system. This CMR is characterised by the least-squares fit $T_1 = (38.4 \pm 1.8) - (13.6 \pm 1.0)(C - T_1)$. This latter fit corresponds to the whole galaxy range, as a break is not distinguishable in this observed CMR. Note that this is so because the brightest galaxies in this sample hardly reach the magnitudes above the break detected in the simulations.

The linear fit to the bright end of the RS in this colour-magnitude plane for the C15 cluster is represented in the bottom left panel of Fig. 1 by a red dotted line, and gives $M_{T_1} = 83.65 - 67.92(C - T_1)$. Its slope clearly differs from the one corresponding to the faint end, which is fit by the relation $M_{T_1} = 0.82 - 12.38(C - T_1)$, shown with a blue solid line. This latter fit is closer to the one applied to the whole RS, for which we obtain $M_{T_1} = 2.19 - 14.62(C - T_1)$. The slope of the fit to the whole RS of the C14_2 cluster is -13.77 (see Table 1) in very good agreement with the observed value -13.6 of the slope for Antlia. Similar results have been found in all the simulated clusters, as can be seen from Table 1. This supports the idea of the universality of the CMR as inferred from observational results (e.g. López-Cruz et al. 2004; de Rijcke et al. 2009).

The detachment of the bright end ($-24 \lesssim M_{T_1} \lesssim -20$) with respect to the linear fit to the faint end is clear for the three massive simulated clusters (C15), although the change of slope in the RS of the less massive clusters (C14) is not so

evident. This is mainly due to the lack of objects in the high luminosity range of C14 clusters and the intrinsic scatter of the relation. Only two small groups (C14_1, C14_2) show a slightly tighter relation at $M_{T_1} \lesssim -20$, where the change of slope becomes perceptible. As mentioned above, this effect is present in some observed CMRs as well. For instance, it can be seen in the CMR of Hydra I cluster presented by Misgeld et al. (2008) (their Figs. 2 and 10), though it is not particularly noticed by the authors. The studies of the Virgo cluster by Janz & Lisker (2009) and of a large sample of local ETGs by Skelton et al. (2009), both based on SDSS data, clearly show a tilt towards bluer colours at the bright end of their CMRs.

We find a very good agreement between the slopes of the observed CMR and the simulated RS, specially for galaxies fainter than the break $M_{T_1}^{\text{break}} \sim -20$. It is remarkable that this global agreement, as well as the tilt of the bright end towards bluer colours, emerge naturally from SAG after calibrating the code to satisfy several other observational constraints simultaneously, as mentioned in Section 2.

3.2 Luminosity-metallicity relation

One of the main properties also affected by the physical processes driving the development of the CMR is the galaxy metallicity. Simulated galaxies that form the RS shown in Fig. 1 are identified by different coloured symbols according to the metallicity range in which they lie. The metallicity of each galaxy is characterised by the iron abundance of its stellar component by using the index $[\text{Fe}/\text{H}]$, where we are considering the solar value of iron abundance by number $(\text{Fe}/\text{H})_{\odot} = 2.82 \times 10^{-5}$ (Asplund et al. 2005). We can see that galaxies at the bright end are the most metal rich ones with $[\text{Fe}/\text{H}] \gtrsim -0.25$, some of them reaching values as high as $[\text{Fe}/\text{H}] \approx 0.43$; the mean value of their metallicity distribution is $\langle [\text{Fe}/\text{H}] \rangle = -0.03 \pm 0.05$. As we move down along the RS, galaxies become fainter, bluer and less chemically enriched. This plot clearly reflects the fact that the RS can be interpreted as a mass-metallicity relation.

We can further test whether a luminosity-metallicity relation is present. In the upper panel of Fig. 2, we show this relation for the same simulated galaxies that form the RS of the C15_3 cluster shown in Fig. 1. In order to compare our results with observed data, we include $[\text{Fe}/\text{H}]$ abundances of early-type galaxies belonging to the NGC 5044

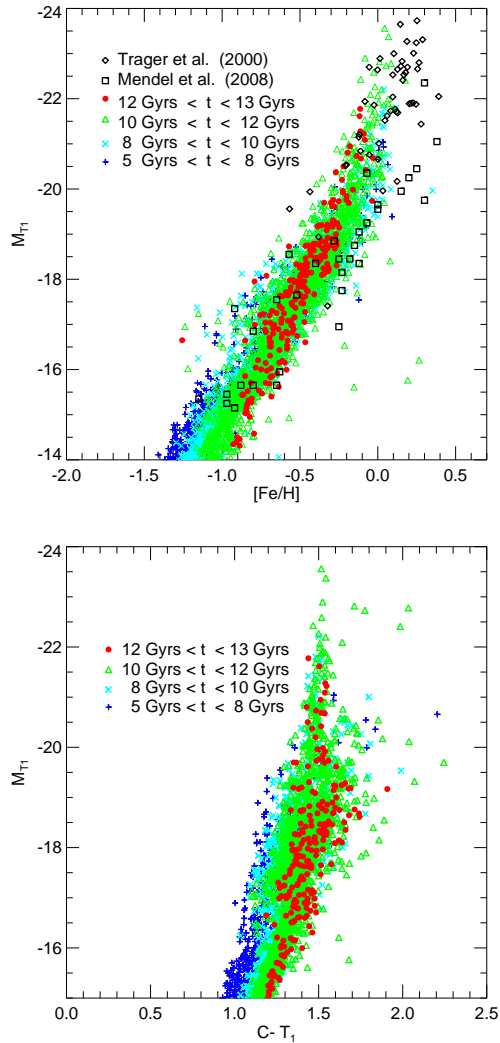


Figure 2. Top panel: Luminosity-metallicity relation for the same simulated galaxies in the RS of the C15_3 cluster shown in Fig. 1. Differently coloured symbols identify galaxies within different ranges of age; black open diamonds represent the $[Fe/H]$ abundances of early-type galaxies belonging to the sample described in Trager et al. (2000), whereas black open squares correspond to galaxies in the NGC 5044 group (Mendel et al. 2009). Bottom panel: RS of simulated galaxies in the magnitude plane T_1 vs. $(C - T_1)$ colour-coded according to the range of ages in which they lie.

group (Mendel et al. 2009), and of a sample described in Trager et al. (2000). The latter contains cluster members (six of the Virgo cluster, eleven of the Fornax clusters, one of the rich cluster Abell 194), but most of the galaxies are in small groups of varying richness. The metallicity of this set of galaxies were re-determined by Trager et al. (2008); $[Fe/H]$ abundances are then obtained from these metallicity values using a transformation given by Trager et al. (2000) (see their Eq. 1). In all cases, we have transformed the absolute magnitudes to the T_1 band through the relations of Fukugita et al. (1995). As can be seen, the observed values, which cover a wide range of magnitudes and abundances, overlap the simulated relation. The agreement is particularly

good for galaxies in the faint end of the RS ($M_{T_1} \gtrsim -20$), although we note that the observed abundances of some galaxies in the bright end are slightly larger than those obtained from our model. This discrepancy may be due to the fact that most of the galaxies in the observed sample are in relatively low-density environments, having different SF and enrichment histories than those residing in massive clusters. The fact that the metallicities of galaxies at $z = 0$ satisfy observational constraints is particularly relevant for our study. It supports the use of the chemical history of galaxies as a tool to help understand the development of the RS and its special feature at the bright end.

Galaxies in the luminosity-metallicity relation of Fig. 2 have been colour-coded according to the range of ages in which they lie. Ages have been estimated considering the stellar mass weighted mean of the birth-time of each single stellar population. A clear correlation between age and metallicity is evident for the least luminous galaxies ($M_{T_1} \gtrsim -16$). Younger galaxies are more metal poor, lying on the left side of the luminosity-metallicity relation, while older galaxies have higher iron abundances being located towards the right. As we move to brighter galaxies along this relation, ages and metallicity become anticorrelated, consistent with the trend found by Gallazzi et al. (2006) for galaxies in the SDSS at fixed velocity dispersion. This anticorrelation might explain the modest scatter of the bright end of the CMR (Trager et al. 2000), which is characterized by a negligible spread in age, also consistent with observational results by Gallazzi et al. (2006). Most galaxies in the bright end of our simulated RS share very similar ages ($1.0 \times 10^{10} \text{ yr} < t < 1.2 \times 10^{10} \text{ yr}$). This can be seen in the lower panel of Fig. 2, where galaxies along the RS in the T_1 vs. $(C - T_1)$ plane are identified with different coloured symbols according to their age. From this figure, it is clear that, in the faint end, the scatter in colour about the RS for a fixed luminosity is caused entirely by age variations, as assumed by Bernardi et al. (2005), where younger galaxies correlate with bluer colours. As we move to higher luminosities, galaxies of a given age become redder because they are more metal rich. The effect of age differences on the final colours of galaxies in the bright end of the RS is completely negligible (see fig. 1 of Bruzual & Charlot 2003), and we can attribute to metallicity effects the behaviour of the galaxies in the bright-end of the RS. In the following, we analyze the physical reasons that make the old galaxies in the bright end reach an upper limit in metallicity. Our aim is to demonstrate that this metallicity effect is the responsible of the colours achieved by massive galaxies which are bluer than those that would be obtained from an extrapolation of the faint end of the RS.

4 PHYSICAL PROCESSES INVOLVED IN THE DEVELOPMENT OF THE RS

The galactic properties that determine the RS, that is, masses and metallicities, are the result of a complex combination of different physical processes involved in the formation and evolution of galaxies. Thus, in order to identify which mechanisms are responsible for the different features of the RS, and in particular the break at the bright end, we track the evolution of the masses and metallicities of

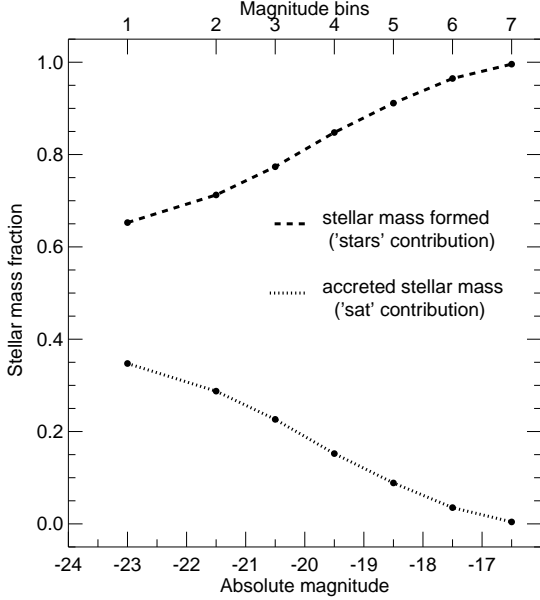


Figure 3. Stellar mass fractions of ‘stars’ and ‘sat’ contributions reached at $z = 0$ by galaxies in the C15 clusters for the different magnitude bins.

the stars added to each galaxy by different processes: quiescent star formation from the cold gas available in the galaxy disc, starbursts during mergers and disc instability events, and the stellar mass accreted from satellite galaxies during mergers.

In the following, the stellar mass generated during any type of star formation event is denoted as ‘stars’, while the stellar mass accreted during mergers, already present in the satellite galaxy, is referred to as ‘sat’. Thus, ‘stars’ and ‘sat’ indicate the class of stellar ‘component’ contributed by a given ‘process’. Hence, the stellar mass of a galaxy g at a certain redshift z that results from the addition of a certain stellar component is denoted by $SM_{g,z}^{\text{proc, comp}}$.

Therefore, we consider a set of variables that take into account the different contributions of stellar mass to a given galaxy, according to the process involved. Specifically,

- (i) stellar mass from quiescent star formation:

- $SM_{g,z}^{\text{quiescent, stars}}$

- (ii) stellar mass from disc instability events:

- $SM_{g,z}^{\text{disc, stars}}$

- (iii) stellar mass from merger events:

- $SM_{g,z}^{\text{minor dry, sat}}$
- $SM_{g,z}^{\text{minor wet, sat}}$
- $SM_{g,z}^{\text{minor wet, stars}}$
- $SM_{g,z}^{\text{major dry, sat}}$
- $SM_{g,z}^{\text{major dry, stars}}$
- $SM_{g,z}^{\text{major wet, sat}}$
- $SM_{g,z}^{\text{major wet, stars}}$

With all these separate variables, we track the mass assembly history of galaxies and the evolution with redshift of the stellar mass fractions contributed by the different processes. Similar variables are defined to follow the evolution

of the metallicities of galaxies, given by the ratio Fe/H . For each process considered, we keep track of the mass of Fe and H received by a galaxy from formed and/or accreted stars at a given redshift as a result of a certain process; thus, we have the quantities $\text{Fe}_{g,z}^{\text{proc, comp}}$ and $\text{H}_{g,z}^{\text{proc, comp}}$, respectively. In order to achieve a better visualization of the mechanisms that determine the properties of galaxies along the RS, we divide the simulated RS into six bins of one magnitude from $M_{T_1} = -16$ to $M_{T_1} = -22$, and a seventh one from $M_{T_1} = -22$ to $M_{T_1} = -24$. This last bin comprises two magnitudes to improve the statistic analysis, in view of the low number of very luminous galaxies in all simulated clusters. Thus, bin = 1 and bin = 7 correspond to the magnitude ranges $-24 < M_{T_1} \leq -22$ and $-17 < M_{T_1} \leq -16$, respectively. We analyze the evolution with redshift of the fractions of stellar mass contributed by different processes to galaxies in a given magnitude bin, and of their mean metallicity. To this aim, we define several quantities that are included in these calculations.

The total mass of stars acquired by galaxies in a magnitude bin b at redshift z arising from a given component contributed by a particular process is:

$$SM_{b,z}^{\text{proc, comp}} = \sum_{g=1}^{N_{b,z}} SM_{g,z}^{\text{proc, comp}}, \quad (2)$$

where $N_{b,z}$ is the number of galaxies within each bin b at each snapshot of the simulation characterized by a redshift z . Then, considering the combined contribution of the two stellar components (‘stars’ and ‘sat’) by any given process, we have

$$SM_{b,z}^{\text{proc}} = SM_{b,z}^{\text{proc, stars}} + SM_{b,z}^{\text{proc, sat}}. \quad (3)$$

Finally, the total stellar mass acquired by all galaxies in a given magnitude bin that results from the contribution of all the involved processes is

$$SM_{b,z}^{(\text{i})+(\text{ii})+(\text{iii})} = \sum_{\text{proc}=1}^{N_{\text{proc}}} SM_{b,z}^{\text{proc}}, \quad (4)$$

where N_{proc} is the total number of processes considered grouped in the sets (i), (ii) and (iii), as described previously.

In the following, all results shown correspond to averages over the three C15 clusters; error bars are not included in the plots because they are extremely small. We have also evaluated the situation considering C14 clusters.

4.1 Evolution of stellar mass fractions

Taking into account the definitions given above, we estimate the fraction of stellar mass accreted by galaxies in each magnitude bin at a given z resulting from the contribution of each of the processes considered, distinguishing between the two different components, as

$$\text{SMFrac}_{b,z}^{\text{proc, comp}} = \frac{SM_{b,z}^{\text{proc, comp}}}{SM_{b,z}^{(\text{i})+(\text{ii})+(\text{iii})}}. \quad (5)$$

These stellar mass fractions can be grouped according to the aspect we want to analyse.

We first consider the fractions of the stellar mass given by new formed stars, on one hand, and accreted stars, on the

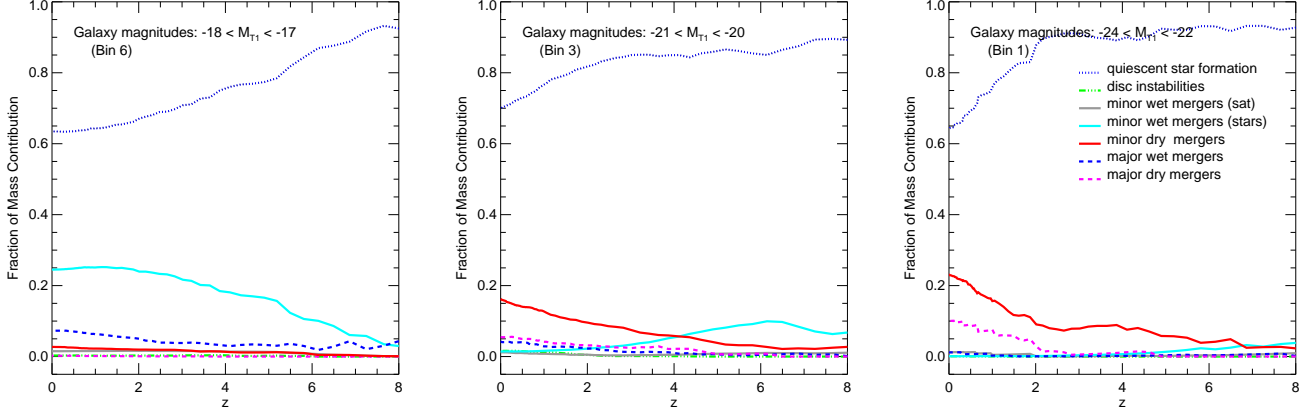


Figure 4. Evolution of the mean stellar mass fractions contributed by different processes for galaxies within magnitude bins 1, 3 and 6, normalized to the total contribution to the stellar mass at each redshift the three C15 clusters are considered. Left panel: galaxies with magnitudes within the range $-18 < M_{T_1} \leq -17$, magnitude bin 6. Middle panel: galaxies with magnitudes within the range $-21 < M_{T_1} \leq -20$, magnitude bin 3 (critical bin). Right panel: galaxies with magnitudes within the range $-24 < M_{T_1} \leq -22$, magnitude bin 1.

other, regardless of the processes that contribute to them. Thus we have

$$\text{SMFrac}_{b,z}^{\text{comp}} = \sum_{\text{proc}=1}^{N_{\text{proc}}} \text{SMFrac}_{b,z}^{\text{proc, comp}}, \quad (6)$$

for the ‘stars’ and ‘sat’ components. The dependence of these fractions with the magnitude bins, in which galaxies along the RS lie, is presented in Fig. 3 for the two components, considering the values of stellar mass reached at $z = 0$. As can be seen, the stellar mass received by all galaxies along the RS is mainly composed by the ‘stars’ contribution ranging from $\sim 95\%$ for the least luminous galaxies ($M_{T_1} \geq -17$, lying in bin 7), to $\sim 65\%$ for the most luminous ones ($M_{T_1} \leq -24$, bin 1). This gradual reduction of the fraction of stellar mass contributed by the stars for the more luminous galaxies occurs at expenses of the accretion of the stellar component of merging satellites (‘sat’ contribution), indicating that mergers become important for the more massive galaxies.

We now analyse the evolution with redshift of the accumulated stellar mass contributions from the different processes, within different magnitudes bins. The evolution of the corresponding mean fractions of stellar mass are shown in Fig. 4 for galaxies with magnitudes corresponding to bins 1, 3 and 6; these fractions are given with respect to the total contribution to the stellar mass of galaxies at the redshifts considered. Although we have taken into account both the ‘stars’ and ‘sat’ components arising from major dry mergers, we found that the contribution of the former to the whole stellar mass of galaxies is negligible. Hence, in the following, we simply refer to this process as ‘major dry merger’, meaning that only the stellar mass from the ‘sat’ component is being considered.

From a first inspection of these plots, we see that quiescent SF appears as the dominant process that contributes to the stellar mass of galaxies within all magnitude bins and at all redshifts. However, we can see that the corresponding stellar mass fractions decrease monotonically with redshift as the cold gas reservoir in each galaxy is exhausted.

The relative contribution of the rest of the processes, broadly grouped in disc instabilities and mergers, change considerably as we move along the RS. The left panel of Fig. 4 shows the mean stellar mass fractions for galaxies with low luminosity ($-18 < M_{T_1} \leq -17$, bin 6). We can clearly see that the second larger contribution to the stellar mass of these galaxies comes from the stars formed during minor wet mergers (i.e. the ‘stars’ component); this mass fraction increases with redshift reaching a value of $\approx 25\%$ per cent at $z \approx 0$ that has already been achieved at $z \approx 2$, indicating that minor wet mergers do not play a significant role since that epoch. These fractions are followed by those corresponding to the contribution of the major wet merger. As we will see, the contribution of this particular process is very small or almost negligible for more luminous galaxies, therefore, for the sake of clarity, we do not split this process in the two different components. The mass contributions provided by disc instabilities and other kind of mergers are negligible.

As we move up along the RS to higher luminosities, the situation changes appreciably. The mass fractions for galaxies in the critical magnitude bin 3, where the detachment of the bright end of the RS from the general linear fit occurs, are shown in the middle panel of Fig. 3. At these magnitudes, the relevant contribution to the stellar mass content (apart from quiescent SF) arises from minor dry mergers, while the relevance of the ‘stars’ component in minor wet mergers decreases considerably from $z \approx 4$, becoming negligible at $z = 0$, in contrast to the behaviour manifested by this process for galaxies in bin 6. We also find a mild contribution of major wet mergers at low redshift. All these merger events are responsible of $\approx 20\%$ of the stellar mass received by galaxies with magnitudes in the range $-21 < M_{T_1} \leq -20$ at $z = 0$.

For the most luminous galaxies ($-24 < M_{T_1} \leq -22$, bin 1), the trend of the mass contribution of minor dry mergers is reinforced with respect to the one shown for bin 3, gaining importance from earlier epochs ($z \approx 6$), and reaching a higher value of $\approx 22\%$ at $z = 0$. The contribution of ma-

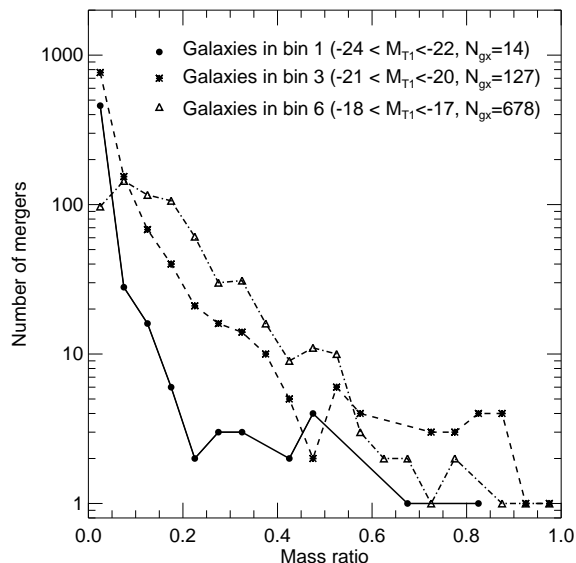


Figure 5. Number of mergers suffered by the galaxies in a C15 cluster through their whole lifetime as a function of the baryonic mass ratio of mergers; different curves correspond to magnitude bins 1, 3 and 6, which contain different number of galaxies.

for dry mergers also increase notably since $z \approx 2$ giving a fraction of $\approx 10\%$ at $z = 0$. Thus, the whole contribution of these two relevant processes at the present epoch leads to a fraction of $\approx 32\%$, consistent with the result shown in Fig. 3.

Although the previous description is based on the mean mass fractions of galaxies in the massive C15 clusters, which clearly show the change in slope of the RS, similar results are obtained for the small simulated clusters C14 (not shown). In the latter, however, statistics become very poor at high luminosities, with only a few objects, if any, in the highest magnitude bin. This general behaviour is in agreement with the scenario inferred by Martínez et al. (2010) from the analysis of galaxies in groups and in the core of X-ray clusters, in which these galaxies populate nearly the same CMR. Their result supports previous works that indicate that the CMR is independent of the environmental overdensity (Hogg et al. 2004; López-Cruz et al. 2004).

4.2 Mass ratio of mergers resolved in the model

The contribution of minor mergers to the stellar mass is relevant for galaxies in all magnitude bins, as it is evident from Fig. 4. The mass ratio of minor mergers that are resolved by the model depends on the mass of the galaxies involved. Given the mass resolution for DM haloes in the N -body/SPH simulations used, a very conservative upper limit for the mass resolution in galaxies would be $\sim 10^9 h^{-1} M_\odot$ (the minimum resolved halo mass times the baryonic fraction), but due to the complex interplay of processes such as gas cooling, feedback and strangulation, we find that our model produces objects with stellar mass as small as $1.5 \times 10^5 h^{-1} M_\odot$. Therefore, the minimum mass ratio resolved in the model (corresponding to the merger of such an

object with a BCG, with stellar mass of $\simeq 1.5 \times 10^{12} h^{-1} M_\odot$ in our simulations) is $\sim 10^{-7}$. However, it is likely that our model is incomplete for such small objects.

Comparing the results of the model with e.g. the observed luminosity function for galaxy clusters (DePropris et al. 2003), it seems our model is complete for galaxies with absolute magnitude < -15 in the b_J -band. This corresponds to galaxies with a mean stellar mass $\simeq 2 \times 10^8 h^{-1} M_\odot$. Consequently, for the case of the BCGs, we expect our model to be complete in mergers with mass ratio $\gtrsim 10^{-4}$. For galaxies in the C15 clusters, the minimum mass ratios resolved in the model are of the order of 4×10^{-5} , 10^{-4} and 6×10^{-3} for bins 1, 3 and 6, respectively. The ratios indeed increase as one considers less luminous galaxies. When selecting the most luminous galaxies in bin 1 in the C14 clusters, the minimum mass ratio is higher but of the same order of magnitude, $\sim 2.5 \times 10^{-5}$.

In general, the number of mergers suffered by galaxies along their whole lifetime increases rather monotonically as mergers of lower mass ratio are considered, as can be seen from Fig. 5, where the results are shown for magnitude bins 1, 3 and 6. Minor mergers (defined as those with mass ratio lower than 0.3; Section 2.3) are dominant for all galaxies along the RS. For the least luminous bin, the maximum is not reached for the least value of the mass ratio, as in the more luminous ones, reflecting the influence of the limit in the mass resolution of the simulations. Each of these bins contains different number of galaxies, as indicated in the plot, being larger for the least luminous one. Taking into account this aspect, the average number of mergers is larger for brighter galaxies.

4.3 Influence of gas fraction thresholds

From the analysis of the stellar mass fractions discussed in Subsection 4.1, it is clear that the evolution of galaxies in the bright end of the RS (those brighter than the critical value ($M_{T1} \approx -20$) is driven by the dry contribution of both minor and major mergers. On the other hand, fainter galaxies are affected by the wet component of mergers.

These conclusions are in agreement with those obtained by Skelton et al. (2009), who find that most of the galaxies in the bright end of the CMR of local early-type galaxies have undergone dry mergers, in contrast to faint galaxies. Their results are based on a simplified model that isolates the effects of the dry merging in the colours of the RS galaxies. The merger histories and gas fractions of galaxies are extracted from the semi-analytic model of Somerville et al. (2008). Their model is able to reproduce the change of slope in the bright end of the CMR as seen in local early-type galaxies from the SDSS. Skelton et al. affirm that this change in slope, and the magnitude at which the break occurs, depend strongly on the assumption of the gas fraction threshold below which mergers are considered dry. This threshold is allowed to vary between 10 and 30 per cent.

In our model, on the contrary, the tilt of the RS towards bluer colours has only a weak dependence on the gas thresholds adopted to distinguish between wet and dry mergers (defined in Section 2.3 as $f_{\text{gas,minor}}$ and $f_{\text{gas,major}}$ for the minor and major mergers, respectively). The parameter $f_{\text{gas,major}}$ has no influence on the effect of major mergers, because such mergers always lead to the forma-

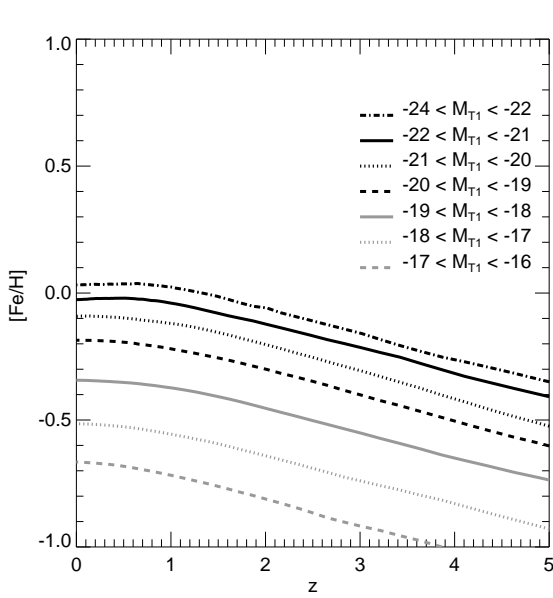


Figure 6. Evolution with redshift of iron abundance of the stellar component of galaxies that at $z = 0$ lie within a given range of magnitudes; metallicity values are a result of the complex combination of all processes included in our model SAG. Averages at each redshift have been estimated considering galaxies in C15 clusters. Different lines represent the mean values for galaxies within different magnitude bins.

tion of a spheroid and the consumption of the cold gas in a starburst, regardless of the amount of gas available in the merging galaxies. The threshold $f_{\text{gas},\text{major}}$ only has the purpose of classifying major mergers as either dry or wet, and thus only affects the percentages of the ‘stars’ and ‘sat’ components contributed by these processes to the stellar mass of galaxies. We have verified that changing this threshold within the range $0.2 \leq f_{\text{gas},\text{major}} \leq 0.6$ results in no significant changes with respect to the results presented in Figure 4, obtained for $f_{\text{gas},\text{major}} = 0.4$. On the other hand, the value $f_{\text{gas},\text{minor}} = 0.6$ for the minor mergers has been tuned together with the rest of the free parameters of the model in order to reproduce several observed galaxy properties, as described in Section 2.3.

We would like to emphasize that our model was not constructed to produce a break in the RS; this arises naturally as a consequence of the physical processes included in the model. In particular, varying the value $f_{\text{gas},\text{major}}$ over the aforementioned range, a break in the bright end of our simulated RS is always present, without any appreciable change in the values of the slope or of the critical break magnitude. In this respect, our findings differ from those of Skelton et al. (2009), who claim to see a strong dependence of the break on the adopted gas threshold; moreover, we do not see a significant dependence from their results (see their Fig. 1). In any case, both our results and those of Skelton et al. (2009) strongly support the fact that the dry contribution of the merger processes are relevant in the formation of the brightest galaxies in the RS, both in field and cluster environments. It has been suggested that dry mergers are expected to only increase the mass of the remnant without changing their colours because there is no associated SF, thus caus-

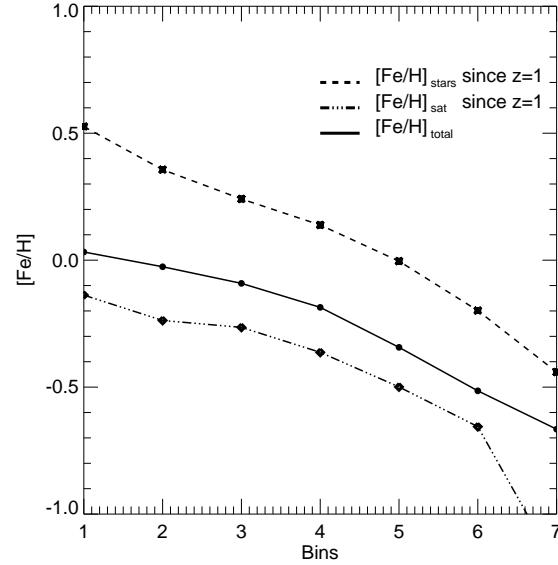
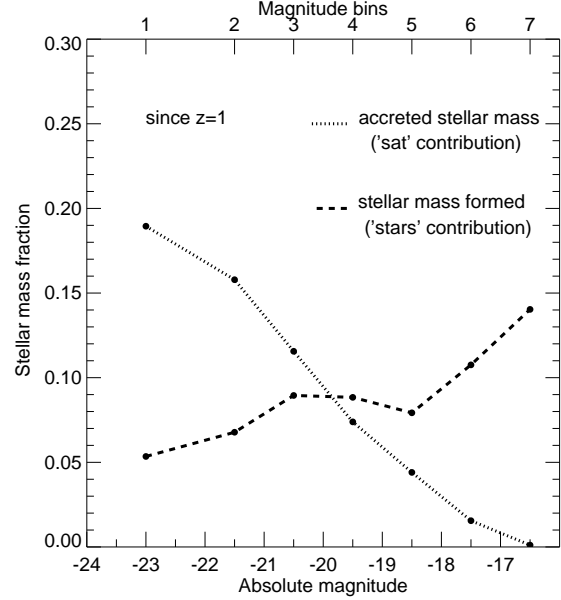


Figure 7. Top panel: stellar mass fractions of ‘stars’ and ‘sat’ contributions accumulated since $z = 1$ for each magnitude bin, normalized with the total stellar mass of galaxies at $z = 0$ within a given bin; galaxies in the C15 clusters are considered. Bottom panel: Average iron abundance of galaxies at $z = 0$ as given by the complete evolution traced by the semi-analytic model (solid line), for galaxies within different magnitude bins, compared with the metallicity of the mass contributed by the stars formed since $z = 1$ (dashed line) and of the stars already present in the satellites accreted since $z = 1$ (dot-dashed line).

ing the detachment of the bright end from the general linear trend (Bernardi et al. 2007; Skelton et al. 2009). In what follows, we explain this claim by means of our detailed model of galaxy formation, focusing on cluster galaxies.

4.4 Metallicity evolution

The evolution of the mean value of the stellar iron abundance of galaxies that at $z = 0$ lie within a given range of magnitudes is shown in Fig. 6. These metallicities are the result of the complete combination of all the processes considered in the semi-analytic code; averages have been estimated for each magnitude bin considering the three C15 clusters. We can see that, regardless of the galaxy magnitude, the mean metallicity of galaxies increases smoothly with redshift, being always higher for the more luminous galaxies. In particular, at $z = 0$, galaxies in the bright end ($M_{T_1} > -20$) reach metallicity values within a narrower range (≈ 0.15 dex) than the rest of the galaxy population. This fact is directly linked with the similar colours that characterize these galaxies making them depart from the general trend of the RS. These chemical abundances seem to be in place since $z = 1$. This is supported by observations of high redshift clusters, which show that the slope and scatter in the CMR for morphologically selected ETGs show little or no evidence of evolution out to $z \approx 1.2$ (Blakeslee et al. 2003; Mei et al. 2006; Jaff et al. 2010).

4.5 Mass assembly and merger rates since $z = 1$

Taking into account that metallicity values of galaxies in the bright end have already been achieved at $z = 1$ (Fig. 6), we consider the accumulated mass contributed from both components ('stars' and 'sat') in the redshift range $0 < z < 1$. The relative contribution of these two components are shown in the top panel of Fig. 7 for galaxies in different magnitude bins. These mass fractions are normalized with the total stellar mass of galaxies at $z = 0$ within a given magnitude bin, because we are interested on the relative importance of the mass accumulated since $z = 1$ to the stellar mass of the galaxy at the present epoch. Note that this stellar mass is a result of the whole evolution traced by the semi-analytic code, including its reduction as a result of the mass recycling arising from stellar evolution. However, by construction, the variables used to analyse the mass fractions shown in Fig. 7 (as well as in Figs. 3 and 4) save the information of the mass of stars born in a galaxy or added to it during merger events, but they are not updated to take into account the recycled mass. This fact specially affects the stellar mass fractions contributed by the mass of new born stars ('stars' component) since $z = 1$, which are shown by the dashed line in the top panel of Fig. 7. As we can see, these fraction ranges from ≈ 0.05 for the brightest galaxies to ≈ 0.15 for the faintest ones. However, they are in fact even lower taking into account that they are normalized with the total stellar mass of galaxies at $z = 0$, which have lost ≈ 35 per cent of their mass as a result of the evolution of stars belonging to the high mass tail of a Salpeter IMF (which is the one adopted in our semi-analytic model).

These fractions of the stellar mass formed in situ since $z = 1$, in which all physical processes contributing with cold gas from which new born stars originate are taken into account, can be compared with estimations done by Kaviraj et al. (2008). They compute the recent star formation (RSF; mass fraction of stars that form in the galaxy within the last 1 Gyr of look-back time in its rest frame) in the high redshift ($0.5 < z < 0.1$) early-type population from

rest-frame UV and optical colours and combine their results with similar studies in the local universe (Kaviraj et al. 2007), thus being able to estimate the star formation history of the early-type population between $z = 0$ and 1. For the range $0.5 < z < 1$, early type galaxies belonging to the RS ($NUV - r > 4$) typically show RSF values less than 5 per cent and the reddest early-types (which are also the most luminous) are virtually quiescent with RSF values of ~ 1 per cent.

On the other hand, Kaviraj et al. (2007) find that the SF activity in the most active ETGs (those in the blue peak of the colour-magnitude distributions) has halved from an average RSF of ~ 11 per cent at $z = 0.7$ to ~ 6 per cent at the present day. From these results, they infer that 10 – 15 per cent of the stellar mass in luminous early-type galaxies ($-23 < M_V < -20.5$) may form after $z = 1$, while less luminous galaxies may form 30 – 60 per cent of their mass within this time-scale. The fractions of the stellar mass formed in situ since $z = 1$ given by our model (dashed line in Fig. 7) are a factor of 2 smaller than these values, within ranges of $\sim 0.05 - 0.09$ and $\sim 0.09 - 0.15$ per cent for galaxies in the bright and faint end of the RS, respectively. This difference is expected, taking into account that we are analysing cluster galaxies where the peak of the star formation takes place at earlier times, while those in the study of Kaviraj et al. (2008) belong to a variety of environments. Thus, our results are in very good agreement with these observational estimates.

The stellar mass fractions contributed by the accreted stellar mass during mergers are not so affected by the definition of the accumulated quantities, since the stellar population of satellites have already suffered from the recycling processes by the time they are accreted, assuming that the bulk of their stars were formed at $z > 1$. Indeed, if a satellite galaxy accreted within the redshift range $0 < z_{\text{merger}} < 1$ is created as early as $z = 7$, then, by the time it merges with the central galaxy it has already lost ≈ 36 per cent of its original mass retaining only the low mass (slowly evolving) stars. Then, the stars that will be added to the central galaxy will evolve very slowly and more than 93% of those stars will still be alive at $z = 0$. Even in the case of a relatively young galaxy created at $z = 2$ and accreted during the time interval $0 < z_{\text{merger}} < 1$, we find that more than 90% of the stellar mass added during the merger is still alive at $z = 0$. Keeping these caveats in mind, we can conclude from Fig. 7 (upper panel) that $\approx 10 - 20$ per cent of the mass of galaxies in the bright end of the RS arises from satellites accreted since $z = 1$, with very few stars being formed in situ.

Observational quantification of the impact of mergers in the mass assembly of early type galaxies yields to larger increments of the mass of galaxies since $z = 1$ with respect to what we have found. However, we have to keep in mind that our results correspond to cluster galaxies, characterized by a faster evolution, as already mentioned. In particular, Lopez-Sanjuan et al. (2010) find that the brightest early-type galaxies increase their mass by about 42 ± 8 per cent as a result of mergers since $z = 1$. They use kinematically confirmed close pairs from the VIMOS VLT deep spectroscopic redshift survey to study the role of minor mergers to mass assembly of normal $L_B \gtrsim L_B^*$ galaxies, which can belong to different environments. The fact that the mass fraction

received by massive early-type galaxies in their sample is a factor of two larger than the one estimated for our brightest galaxies is a consequence of the lower number of mergers that cluster galaxies suffer since $z = 1$.

The estimation of the average number of mergers per red galaxies since $z = 1$ done by Lopez-Sanjuan et al. (2010) is 1.3 ± 0.3 , that is splitted in 0.7 ± 0.1 major mergers and 0.6 ± 0.2 minor ones. Their criterion to separate between minor and major mergers is based on the ratio of B -band luminosity of the merging components which is used as a proxy of mass; minor mergers are characterized by the luminosity ratio ranging from 0.1 to 0.25. In our model, minor mergers are defined as those having mass ratios less than 0.3, without imposing a lower limit. Thus, we find that galaxies in the bright end of the RS ($M_{T_1} \leq -20$) have suffered an average number of mergers of ~ 4.88 since $z = 1$, which is almost four times larger than the value obtained by Lopez-Sanjuan et al. (2010). Therefore, we repeat our estimation restricting to minor mergers with mass ratios larger than 0.1. Thus, we find that the average number of mergers suffered by galaxies in the bright end of the RS is considerably reduced, with ~ 0.33 minor mergers per galaxy. The value is a factor of two smaller than the one inferred by Lopez-Sanjuan et al. (2010), but again, we have to keep in mind that our sample contains cluster galaxies.

The cumulative fraction of stellar mass contributed by minor mergers since $z = 1$ that we compute, ranges from ~ 0.12 to 0.07 , for the most and the least luminous galaxies in the bright end of the RS, respectively, which are in very good agreement with the estimation of 0.1 done by Lopez-Sanjuan et al. (2010). These values have been obtained in the same way as those shown in the upper panel of Fig. 7 but restricting to the contribution of the ‘sat’ component of minor mergers, including those with mass ratio less than 0.1. This indicates that the mass contribution of minor mergers with such a low mass ratio, although being highly numerous, contribute with a very small percentage to the stellar mass of the central galaxy. On the other hand, the average number of major merger suffered by the brightest galaxies in the RS since $z = 1$ is ~ 0.19 , a factor of three smaller than the one obtained by Lopez-Sanjuan et al. (2010), which explains that the mass fraction contributed by all kind of mergers to the brightest galaxies in the RS (~ 0.2) is a factor of two smaller than observed by Lopez-Sanjuan et al. (2010) (~ 0.42). However, this value of the number of major mergers is in better agreement with other empirically determined major merger rates, which indicates that major merger activity in galaxies with masses comparable with the ones in this paper, becomes infrequent after $z = 1$ (e.g. Conselice et al. 2009; Bundy et al. 2009; Jogee et al. 2009).

We also compare our results with those obtained by Nierenberg et al. (2011). They study the spatial distribution of faint satellites of early-type galaxies at intermediate redshifts ($0.1 < z < 0.8$) selected from the GOODS field. Satellites are detected from high resolution HST images considering those that are up to 5.5 magnitudes fainter than the host galaxy and as close as $0''5/2.5$ kpc to the host. The majority of their host galaxies are massive elliptical galaxies with typical stellar masses of $\approx 10^{10.5} M_\odot$ that have on average $1.7^{+0.9}_{-0.8}$ satellites. This inferred satellite number can easily account for the number of minor mergers ($0.4 - 0.5$) that

60 per cent of their host galaxies are expected to undergo in the time span of the study. This number of mergers has been obtained by using the fitting form for the mean merger rate per halo as a function of halo mass, progenitor mass ratio and redshift derived by Fakhouri et al. (2010) from halo merger statistics. Although a bit lower than these inferred values, the result from our model (~ 0.33 minor mergers per galaxies since $z = 1$) is consistent with them.

4.6 Metal contribution since $z = 1$

An interesting aspect of the plot in the lower panel of Fig. 7 is that the contributions of the ‘stars’ and ‘sat’ components cross each other at the break magnitude $M_{T_1} = -20$, clearly indicating that the stellar population accreted during late mergers determines the properties of galaxies in the bright end of the RS. From the discussion related to this plot, we can safely assume that more than 90% of the stellar mass formed and added by mergers since $z = 1$ is still alive at $z = 0$, determining the metallicity and colour of galaxies in the RS at the present epoch. We estimate the metallicity of the stellar mass contributed since $z = 1$ by the these two components, $[\text{Fe}/\text{H}]_{\text{stars}}$ and $[\text{Fe}/\text{H}]_{\text{sat}}$, considering the mass of iron, $\text{Fe}_{g,z}^{\text{proc comp}}$, and hydrogen, $\text{H}_{g,z}^{\text{proc comp}}$, defined in Section 4. The average value of these metallicities for C15 cluster galaxies within different magnitude bins are shown in the lower panel of Fig. 7. They are compared with the average metallicity achieved by the stellar mass of galaxies at $z = 0$ according to the whole evolution traced by the semi-analytic code (solid line), which lies in the range $-0.65 \lesssim [\text{Fe}/\text{H}]_{\text{total}} \lesssim 0.05$ for the least to the most luminous galaxies in the RS. The metallicity of the new stars formed since $z = 1$ (dashed line) ranges from $[\text{Fe}/\text{H}]_{\text{star}} \approx -0.45$ for the least luminous galaxies to ≈ 0.5 . In particular, for galaxies in the bright end of the RS, with magnitudes $-24 \leq M_{T_1} \leq -20$ (bins 1, 2 and 3), the metallicity of the ‘stars’ component is above solar ($0.25 \lesssim [\text{Fe}/\text{H}]_{\text{stars}} \lesssim 0.5$) as the result of the highly chemically enriched cold gas available for star formation in more massive galaxies. However, as we have seen, the mass fraction contributed by processes involving star formation is very low for these galaxies (see top panel of Fig. 7), therefore, these metal contributions hardly affect the metallicity of the whole galaxy. On the other hand, the ‘sat’ component of satellites accreted since $z = 1$ represents an appreciable fraction of the galaxy mass at $z = 0$ for galaxies in the bright end ($\approx 10-20$ per cent), but the values $[\text{Fe}/\text{H}]_{\text{sat}}$ (dashed-dotted line in bottom panel of Fig. 7) are subsolar for galaxies in all magnitude bins, being ≈ 0.15 dex lower than the corresponding galaxy metallicity. Hence, dry mergers help increase the mass of galaxies in the bright end of the RS without considerably affecting their average metallicities. This upper limit in the metallicity achieved by galaxies in the bright end fixes their colour, being bluer than expected if star formation from highly chemically enriched gas were relevant in their final evolution, thus explaining the departure of the bright end of the RS from a linear fit.

4.7 Discussion

Our findings related to the low metallicity of the stellar mass of satellites accreted at low redshifts ($z < 1$), with respect to

the chemical abundances found in the remnant galaxy, are in line with the results of Lagos et al. (2009). They show a clear correlation between the metallicity of galaxies and the mass of their host DM haloes, with central galaxies being more chemically enriched than their surviving satellites. This trend is a direct consequence of the hierarchical clustering process, where more massive galaxies sit in initially higher density peaks and, as a consequence, start to form earlier on average, allowing them to acquire higher amounts of metals.

Our results also support the scenario proposed by Martínez et al. (2010) for the formation of the CMR in massive systems. Their analysis of observational results indicate that the CMR is populated by red ETG that formed the bulk of their stars during the early stages of massive halo assembly, on one hand, and red galaxies that passed most of their lives inhabiting poor groups or the field and fell into massive systems at lower redshifts, on the other. Our study suggests that part of the later population are the satellites intervening in the dry mergers processes, that play a significant role in the late evolution of massive galaxies.

The fact that massive cluster galaxies are fed by minor dry mergers whereas fainter galaxies along the CMR are mainly affected by minor wet ones is due to the influence of the environment in which the host galaxy and their satellites reside. More massive galaxies tend to inhabit denser regions, where it is highly likely that infalling satellites are stripped of their cold gas before the merger as a result of environmental effects. Hence, the modelling of the environmental processes that affect the cold gas content of galaxies could influence our conclusions regarding the fraction of mass received by galaxies from dry or wet mergers. In our model, as in most previous semi-analytic modelling, the hot gas haloes of galaxies are completely and immediately stripped as soon as a galaxy becomes a satellite of a group or cluster. The affected galaxy cannot replenish its cold gas any further, and with a typical SFR it exhausts its cold gas in a few Gyr (Gallagher, Hunter & Bushouse 1989). This process is called ‘strangulation’ (Larson et al. 1980), and provides an explanation for the SFR gradients in clusters (Balogh et al. 2000) and the colour evolution of cluster galaxies (Kodama & Bower 2001). However, recent work (e.g. Weinmann et al. 2006) has shown that, compared to SDSS observations, semi-analytic models produce higher fractions of red satellites. This is likely due to the crude modelling of the removal of the hot gas haloes. If the hot gas is removed more gradually, satellite galaxies can prolong their star formation resulting in bluer colours. It is not known which physical process is actually responsible for the removal of the hot gas, but one likely candidate is ram-pressure stripping (RPS), as shown by McCarthy et al. (2008) and Bekki (2009).

This satellite overquenching problem raises the issue that perhaps the semi-analytic model used overpredicts the number of dry mergers, as satellite galaxies in the model would be too gas-poor. Font et al. (2008) has shown that considering a gradual removal of hot gas by RPS, a better match to the observed fractions of red galaxies is obtained. One would conclude that with such a modification, the number of wet mergers should increase; however, the situation is not so simple. If the gas content of satellite galaxies is regulated by RPS, the colour of the satellite will be bluer as a

result of a more prolonged star formation, but this does not necessarily mean that a higher mass of gas is contributed to the mergers. In the central regions of galaxy clusters the ram-pressure exerted by the ICM is strong enough to significantly affect the gas content of galaxies (Tecce et al. 2010) and by the time the satellite merges with the central, not only its hot gas but also the cold gas could be stripped away by RPS, becoming part of the ICM. Thus, the gas content of the satellite would be mostly removed prior to the merger (Sofue 1994; Grebel, Gallagher & Harbeck 2003) and the number of wet mergers might not increase significantly. We have updated the model described in Tecce et al. (2010) to consider the RPS of the hot gas, and we intend to explore this issue further in a forthcoming paper.

Finally, it is interesting to note that the break magnitude in which there is a change of the slope in the RS ($M_{T_1} \sim -20$), corresponds to a galaxy mass of $M_* \sim 10^{10} h^{-1} M_\odot$, also marks the difference between two regimes in the dependence of metallicity gradients with galaxy mass, as found by Spolaor et al. (2009). Their results suggest that cluster galaxies above the mentioned mass threshold might have formed initially by mergers of gas rich disc galaxies and then subsequently evolved via dry merger events, in concordance with our findings.

5 SUMMARY AND CONCLUSIONS

In this work we have studied the physical processes responsible for the detachment of the bright end of the RS of cluster galaxies from the linear fit determined by less luminous galaxies. The RS is constructed by selecting galaxies according to the empirical redshift-dependent criterion given by Bell et al. (2004) to separate the blue and red sequences in the colour-magnitude diagram. We use the semi-analytic model of galaxy formation and evolution SAG (Lagos et al. 2008; Tecce et al. 2010), combined with cosmological non-radiative *N*-Body/SPH simulations of galaxy clusters in a concordance Λ Cold Dark Matter universe. We consider two sets of simulated clusters with virial masses in the ranges $\simeq (1.1 - 1.2) \times 10^{14} h^{-1} M_\odot$ (C14 clusters) and $\simeq (1.3 - 2.3) \times 10^{15} h^{-1} M_\odot$ (C15 clusters).

We find a very good agreement between the general trends of the simulated RS and observed CMR of ETGs in four different colour-magnitude planes. The simulated relation presents a break at approximately the same magnitude in the different systems ($M_R^{\text{break}} \sim M_V^{\text{break}} \sim M_{T_1}^{\text{break}} \approx -20$, galaxy mass of $\sim 10^{10} M_\odot$), with more luminous galaxies having almost constant colours (Washington $C - T_1 \approx 1.5$) (see Fig. 1) instead of following the linear trend inferred from the less luminous ones.

This aspect is consistent with a non-linear fit found from different set of observations (Baldry et al. 2006; Janz & Lisker 2009; Skelton et al. 2009). The change of slope in the bright end of the RS emerges naturally from our model once it has been calibrated to satisfy several observational constraints simultaneously. One of the observational relationships that is closely followed by the simulated galaxies is the luminosity-metallicity relation (see Fig. 2). This fact supports the use of the chemical history of galaxies as a tool to help understand the development of the RS and its break at the bright end.

Thus, we focus on the analysis of the mass and metals contributed to each galaxy by different physical processes: quiescent star formation, and starbursts during disc instability events and mergers. We study the mean properties of galaxies in seven different magnitude bins; galaxies are grouped according to their M_{T_1} magnitudes. From the analysis of the accumulated stellar mass contributed by different processes, we obtain information about the way in which their relative importance change with redshift, for galaxies in a given magnitude bin, and the dependence of their relevance with galaxy luminosity. We find that:

- Quiescent SF appears as the dominant process that contributes to the stellar mass of galaxies within all magnitude bins and at all redshifts. The corresponding stellar mass fractions decrease monotonically with redshift as the cold gas reservoir in each galaxy is exhausted.
- Galaxies with low luminosity ($-18 < M_{T_1} \leq -17$, bin 6) receive a large contribution from the stars formed during minor and major wet mergers, with the former processes giving place to a larger mass fraction, which increases with redshift and reaches a value of ≈ 25 per cent at $z \approx 0$. This value has already been achieved at $z \approx 2$, indicating that minor wet mergers do not play a significant role since that epoch.
- The most luminous galaxies ($-24 < M_{T_1} \leq -22$, bin 1) have a considerable contribution from minor dry mergers, which become important since $z \approx 6$; the corresponding mass fraction reaches a value of ≈ 22 per cent at $z = 0$. The contribution of major dry mergers is also relevant for these galaxies since $z \approx 2$, giving a fraction of ≈ 10 per cent at $z = 0$.
- The transition between the relative importance of the contribution of wet and dry mergers occurs for galaxies within the range of magnitudes ($-21 < M_{T_1} \leq -20$, bin 3; $M_\star \sim 10^{10} M_\odot$), that is, galaxies characterized by the break magnitude, where the detachment towards bluer colours in the RS takes place. At these magnitudes, minor dry mergers start to gain importance, while the relevance of the stars formed during starbursts in minor wet mergers decreases considerably from $z \approx 4$, becoming negligible at $z = 0$, in contrast to the behaviour manifested by this process for the least luminous galaxies (bin 6). We also find a mild contribution of major wet mergers at low redshifts. All these merger events are responsible of ≈ 20 per cent of the total mass received by galaxies.

From the analysis of the relative importance of the stellar mass fractions contributed by different processes, it is clear that the evolution of galaxies at the bright end of the RS is driven by the dry contribution of both minor and major mergers, while fainter galaxies are affected by the wet component of mergers. This situation is already established at $z \approx 1$. The metallicities of galaxies in the bright end do not change since that redshift, although a mild increase is detected for lower luminous galaxies where star formation from chemically enriched gas keeps taking place.

Considering the mass accumulated since $z = 1$ from both the stars formed in situ and the stellar mass already present in the accreted satellites, we find that the latter represents a fraction of the present stellar mass of galaxies in the bright end of the RS that ranges between ≈ 10 and 20 per cent. This fraction is larger than the fraction of stars

formed during recent star formation. Although the metallicity of the stars formed since $z \approx 1$ is high ($\approx 0.2 - 0.5$ dex above the mean iron abundances of galaxies at $z = 0$, see Fig. 7, bottom panel), their mass contribution is so low (≈ 0.05) that they do not affect the mean metallicity of galaxies. On the contrary, dry mergers provide a higher fraction of stellar mass than that generated by recent SF but with low content of metals (≈ 0.2 dex below the mean metallicity of galaxies) thus, their contribution only increase the stellar mass of galaxies without changing their mean metallicities. Hence, galaxies in the bright end, which have negligible star formation activity since $z \approx 1$, reach an upper limit in their abundances that in turn fixes their colours, taking into account the small spread in age of these systems. The departure of the bright end of the RS from a linear fit can be explained by the effect of the contribution of minor and major dry mergers, which increase the mass/luminosity of the galaxies but without changing their colours.

These conclusions are valid for both high and low mass galaxy clusters. We have demonstrated that the local properties of galaxies on the RS seem to be established since $z \approx 1$. A detailed analysis of the features of the RS, such as its dependence with environment and redshift, will be addressed in a series of forthcoming papers.

6 ACKNOWLEDGEMENTS

We are very grateful to the anonymous referee for a comprehensive and insightful report which helped to improve this paper. We warmly thank Marcelo M. Miller Bertolami and Nelson D. Padilla for largely contributing with useful suggestions and comments. We thank Klaus Dolag for making the simulations available to us, and Scott Trager for kindly providing us his observational data on ETGs. We appreciate the technical support offered by Ruben E. Martínez, Pablo Santa María and Cristian Vega. This work was supported by Consejo Nacional de Investigaciones Científicas y Técnicas, Agencia de Promoción Científica y Tecnológica, National University of La Plata, Argentina and Institute of Astrophysics La Plata (IALP).

REFERENCES

- Adelman-McCarthy J., et al., 2008, *ApJS*, 175, 297
- Asplund M., Grevesse N., Sauval A. J., 2005, in T.G. Barnes III, F.N. Bash, eds, *ASP Conf. Ser. Vol. 36, Cosmic Abundances as Records of Stellar Evolution and Nucleosynthesis*. Astron. Soc. Pac., San Francisco, p. 25
- Baldry I. K., Glazebrook K., Brinkmann J., Ivezić Z., Lupton R. H., Nichol R. C., Szalay A. S., 2004, *ApJ*, 600, 681
- Baldry I. K., Balogh M. L., Bower R. G., Glazebrook K., Nichol R. C., Bamford S. P., Budavari T., 2006, *MNRAS*, 373, 469
- Balogh M. L., Navarro J. F., Morris S. L., 2000, *ApJ*, 540, 113
- Bezanson R., van Dokkum P. G., Tal T., Marchesini D., Kriek M., Franx M., Coppi P., 2009, *ApJ*, 697, 1290
- Bournaud F., Jog C. J., Combes F., 2007, *A&A*, 476, 1179
- Bekki K., 2009, *MNRAS*, 399, 2221

- Bell F. E., Wolf C., Meisenheimer K., Rix H.-W. et al., 2004, *ApJ*, 608, 752
- Bell F. E., Naab T., McIntosh D. H. et al., 2006, *ApJ*, 640, 241
- Bell F. E., Phleps S., Somerville R., Wolf C., Borch A., Meisenheimer K., 2006, *ApJ*, 652, 270
- Bernardi M., Hyde J. B., Sheth R. K., Miller J. C., Nichol R. C., 2007, *ApJ*, 133, 1741
- Bernardi M., Sheth R. K., Nichol R. C., Schneider D. P., Brinkmann J., 2005, *AJ*, 129, 61
- Bernardi M., 2009, *MNRAS*, 395, 1491
- Bernardi M., Roche N., Shankar F., Sheth R. K., 2010, *MNRAS*, submitted (arXiv:1005.3770)
- Bessell M. S., 2001, *PASP*, 113, 66
- Bower R., Lucey J., Ellis R., 1992, *MNRAS*, 254, 601
- Bower R. G., Kodama T., Terlevich A., 1998, *MNRAS*, 299, 1193
- Blakeslee J. P., Franx M., Postman M., Rosati P., Holden B., Illingworth G. D., Ford H. C., Cross N. J. G., et al., 2003, *ApJL*, 596, 143
- Bruzual G., Charlot S., 2003, *MNRAS*, 344, 1000
- Bundy K., Fukugita M., Ellis R. S., Targett T. A., Belli S., Kodama T., 2009, *ApJ*, 697, 1369
- Cappellari Michele; di Serego Alighieri S., Cimatti A., *ApJL*, 2009, 704, 34
- Cenarro A. J., Trujillo I., 2009, *ApJL*, 696, 43
- Conselice C., 2006, *MNRAS*, 373, 1389
- Conselice C., Gallagher J. S., Wyse R. F., 2003, *AJ*, 125, 66
- Conselice C., Yang C., Bluck A. F., 2009, *MNRAS*, 394, 1956
- Cora S. A., 2006, *MNRAS*, 368, 1540
- Croton D. J., Springel V., White S. D. M., et al., 2006, *MNRAS*, 365, 11
- de Vaucouleurs G., 1961, *ApJS*, 5, 233
- Daddi E., Renzini A., Pirzkal N., et al., 2005, *ApJ*, 626, 680
- De Lucia G., Blaizot J., 2007, *MNRAS*, 375, 2
- De Propris R., Colless M., Driver S. P., Couch W., Peacock J. A., Baldry I., Baugh C. M., Bland-Hawthorn J., et al., 2003, *MNRAS*, 342, 725
- Dirsch B., Richtler T., Bassino L.P., 2003, *A&A*, 408, 929
- Dolag K., Vazza F., Brunetti G., Tormen G., 2005, *MNRAS*, 364, 753
- de Rijcke S., Penny S. J., Conselice C. J., Valcke S., Held E. V., 2009, *MNRAS*, 393, 798
- Eliche-Moral M., Prieto M., Gallego J., Zamorano J., 2010, *ApJ*, submitted (arXiv:1003.0686)
- Fan L., Lapi A., Bressan A., Bernardi M., De Zotti G., Danese L., 2010, *ApJ*, 718, 1460
- Fakhouri O., Ma C.-P., Boylan-Kolchin M., 2010, *MNRAS*, 406, 2267
- Ferrarese L., Coté P., Jordan A. et al., 2006, *ApJS*, 164, 334
- Font A. S. et al., 2008, *MNRAS*, 389, 1619
- Forbes D., Forte J. C., 2001, *MNRAS*, 322, 257
- Forte J. C., Faifer F. R., Geisler D., 2007, *MNRAS*, 382, 1947
- Fukugita M., Shimasaku K., Ichikawa T., 1995, *PASP*, 107, 945
- Gallagher J., Hunter D., Bushouse H., 1989, *AJ*, 97, 700
- Gallazzi A., Charlot S., Brinchmann J., White S. D. M., 2006, *MNRAS*, 370, 1106
- Geisler D., 1996, *AJ*, 111, 480
- Grebel E. K., Gallagher J. S. III, Harbeck D., 2003, *AJ*, 125, 1926
- Harris W. E., Harris G. L., 2002, *AJ*, 123, 3108
- Hernquist, L., Mihos, J. C., 1995, *ApJ*, 448, 41H
- Hilker M., Mieske S., Infante L., 2003, *A&A*, 397, L9
- Hogg, D. W., et al. 2004, *ApJL*, 601, L29
- Hopkins P. F., Hernquist L., Cox T. J., Keres D., Wuyts S., 2009, *ApJ*, 691, 1424
- Jaff, Y. L., Aragon-Salamanca A., De Lucia G., Jablonka P., Rudnick G., Saglia R., Zaritsky D., 2010, *MNRAS*, in press (arXiv:1007.1425)
- Janz J., Lisker T., 2009, *ApJ*, 696, L102
- Janz J., Lisker T., 2008, *ApJ*, 689, L25
- Jogee S., Miller S. H., Penner K., et al., 2009, *ApJ*, 697, 1971
- Kaviraj S., Devriendt J. E. G., Ferreras I., Yi S. K., 2005, *MNRAS*, 360, 60
- Kaviraj S., Schawinski K., Devriendt J. E. G., Ferreras I., Khochfar S., Yoon S.-J., Yi S. K., Deharveng J.-M., et al., 2007, *APJS*, 173, 619
- Kaviraj S., Khochfar S., Schawinski K., Yi S. K., Gawiser E., et al., 2008, *MNRAS*, 388, 67
- Kaviraj S., Tan K.-M., Ellis R. S., Silk J., 2011, *MNRAS*, 411, 2148
- Karick A. M., Drinkwater M. J., Gregg M., 2003, *MNRAS*, 344, 188
- Kauffmann G., Colberg J. M., Diaferio A., White S. D. M., 1999, *MNRAS*, 303, 188
- Kawata D., Mulchaey J. S., 2008, *ApJ*, 672, L103
- Khochfar S., Burkert A., 2003, *ApJL*, 597, 117
- Khochfar S., Burkert A., 2006, *A&A*, 445, 403
- Khochfar S., Silk J., 2006, *ApJ*, 648, L21
- Kodama T., Bower R., 2001, *MNRAS*, 321, 18
- Lagos C., Cora S. A., Padilla N. D., 2008, *MNRAS*, 388, 587
- Lagos C., Padilla N. D., Cora S. A., 2009, *MNRAS*, 397, L31
- Lanzoni B., Guiderdoni B., Mamon G. A., Devriendt J., Hatton S., 2005, *MNRAS*, 361, 369
- Larson R. B., Tinsley B. M., Cadwell C. N., 1980, *ApJ*, 237, 692
- Lin L., Cooper M. C., Jian H.-Y. et al., 2010, *ApJ*, 718, 1158
- Lisker T., Grebel E. K., Binggeli B., 2008, *AJ*, 135, 380
- Lopez-Sanjuan, C., Le Favre, O., de Ravel, L., Cucciati, O., Ilbert, O., Tresse, L., et al. 2010, accepted for publication in *A&A*
- Liu F. S., Mao S., Deng Z. G., Xia X. Y., Wen Z. L., 2010, *MNRAS*, 396, 2003
- López-Cruz O., Barkhouse W. A., Yee H. K. C., 2004, *ApJ*, 614, 679
- Malbon R. K., Baugh C. M., Frenk C. S., Lacey C. G., 2007, *MNRAS*, 382, 1394
- Mancini C., Daddi E., Renzini A., Salimi F., McCracken H. J., Cimatti A., Onodera M., Salvato M., et al., 2010, *MNRAS*, 401, 933
- Martinez H. J., Coenda V., Muriel H., *MNRAS*, 403, 748
- Mei S., Holden B., Blakeslee J. P., Ford H. C., Franx M., Homeier N. L., Illingworth G. D., Jee M. J., et al., 2009, *APJ*, 690, 42

- Menci N., Rosati P., Gobat R., Strazzullo V., Rettura A., Mei S., Demarco R., 2008, *ApJ*, 685, 863
- McCarthy I. G. et al., 2008, *MNRAS*, 383, 593
- McIntosh D. H., Guo Y., Hertzberg J., Katz N., Mo H. J., van den Bosch F. C., Yang X., 2008, *MNRAS*, 388, 1537
- Mei S., Holden B. P., Blakeslee J. P., Rosati P., Postman M., Jee M. J., Rettura A., Sirianni M., et al., 2006, *ApJ*, 644, 759
- Mendel J. T., Proctor R. N., Rasmussen J., Brough S., Forbes D. A., 2009, 396, 2103
- Mieske S., Hilker M., Infante L., Mendes de Oliveira C., 2007, *A&A*, 463, 503
- Misgeld I., Mieske S., Hilker M., 2008, *A&A*, 486, 697
- Misgeld I., Hilker M., Mieske S., 2009, *A&A*, 496, 683
- Moore B., Lake G., Quinn T., Stadel J., 1999, *MNRAS*, 304, 465
- Naab T., Johansson P. H., Ostriker J. P., Efstathiou G., 2007, *ApJ*, 658, 710
- Naab T., Johansson P. H., Ostriker J. P., 2009, *ApJ*, 699, L178
- Nakazawa K., Makishima K., Fukazawa Y., Tamura T., 2000, *PASJ*, 52, 623
- Nierenberg, A. M.; Auger, M. W.; Treu, T.; Marshall, P. J.; Fassnacht, C. D., 2011, *ApJ*, 731, 44N
- Pedersen K., Yoshii Y., Sommer-Larsen J., 1997, *ApJ*, 485, L17
- Reda F., Forbes D., Beasley M., O’Sullivan E., Goudfrooij P., 2004, *MNRAS*, 354, 851
- Reda F., Forbes D., Hau G., 2005, *MNRAS*, 360, 693
- Robaina A. R., Bell E. F., van der Wel A., Somerville R. S., Skelton R. E., McIntosh D. H., Meisenheimer K., Wolf C., 2010, *ApJ*, 719, 844
- Roediger E., 2009, *AN*, 330, 888
- Romeo A. D., Napolitano N. R., Covone G., Sommer-Larsen J., Antonuccio-Delogu V., Capaccioli M., 2008, *MNRAS*, 389, 13
- Ruszkowski M., Springel V., 2009, *ApJ*, 696, 1094
- Sandage A., Visvanathan N., 1978, *ApJ*, 223, 70
- Saro A., Borgani S., Tornatore L., Dolag K., Murante G., Biviano A., Calura F., Charlot S., 2006, *MNRAS*, 373, 397
- Secker J., Harris W. E., Plummer J. D., 1997, *PASP*, 109, 1377
- Skelton R., Bell E., Somerville R., 2009, *ApJ*, 699, L9
- Smith Castelli A. V., Bassino L. P., Richtler T., Cellone S., Aruta C., Infante L., 2008, *MNRAS*, 386, 2311
- Sofue Y., 1994, *ApJ*, 423, 207
- Somerville R.S., Hopkins P. F., Cox T. J., Robertson B. E., Hernquist L., 2008, *MNRAS*, 391, 481
- Springel V., White S., Tormen G., Kauffmann G., 2001, *MNRAS*, 328, 726
- Springel V., 2005, *MNRAS*, 364, 1105
- Springel V., White S. D. M., Jenkins A. et al., 2005, *Natur*, 435, 629
- Spolaor M., Proctor R. N., Forbes D. A., Couch W. J., 2009, *ApJL*, 691, 138
- Stott J. P., Pimblet K. A., Edge A. C., Smith G. P., Wardlow J. L., 2009, *MNRAS*, 394, 2098
- Tecce T. E., Cora S. A., Tissera P. B., Abadi M. G., Lagos C. del P., 2010, *MNRAS*, 408, 2008
- Tormen G., Bouchet F., White S. D. M., 1997, *MNRAS*, 286, 865
- Trager S. C., Faber S. M., Worthey G., Gonzalez J. J., 2000a, *AJ*, 120, 165
- Trager S. C., Faber S. M., Dressler A., 2008, *MNRAS*, 386, 715
- van der Wel A., Bell E. F., van den Bosch F. C., Gallazzi A., Rix H.-W., 2009, *ApJ*, 698, 1232
- Visvanathan N., Sandage A., 1977, *ApJ*, 216, 214
- Whitaker K. E., van Dokkum P. G., 2008, *ApJL*, 676, 105
- van Dokkum P. G., Whitaker K. E., Brammer G., Franx M., Kriek M., Labbe I., Marchesini D., Quadri R., et al., 2010, *ApJ*, 709, 1018
- Weinmann S. M., van den Bosch F. C., Yang X., Mo H. J., 2006, *MNRAS*, 366, 2
- Yoshida N., Sheth R. K., Diaferio A., 2001, *MNRAS*, 328, 669